Rapid #: -25336847

CROSS REF ID: **5580187610005946**

LENDER: **GZO (University of Wisconsin, Oshkosh) :: Polk Library**

BORROWER: **FER (Embry Riddle Aeronautical University) :: Hunt Library**

TYPE:	Book Chapter
BOOK TITLE:	Handbook of Marine Craft Hydrodynamics and Motion Control
USER BOOK TITLE:	Handbook of Marine Craft Hydrodynamics and Motion Control
CHAPTER TITLE:	Chapter 7: Models for Ships, Offshore Structures and Underwater Vehicles
BOOK AUTHOR:	Fossen, Thor I
EDITION:	1. Aufl.
VOLUME:	
PUBLISHER:	Wiley
YEAR:	2011
PAGES:	133 - 186
ISBN:	9781119991496
LCCN:	
OCLC #:	729726228

Processed by RapidX: 10/1/2025 7:37:36 AM

7

Models for Ships, Offshore Structures and Underwater Vehicles

This chapter presents hydrodynamic models for ships, offshore structures and underwater vehicles. The foundation for the models are the kinematic equations (Chapter 2), rigid-body kinetics (Chapter 3), hydrostatics (Chapter 4), seakeeping theory (Chapter 5) and maneuvering theory (Chapter 6). Results from these chapters are combined to obtain 1 DOF heading autopilot models, 3 DOF maneuvering and DP models, 4 DOF maneuvering models that include roll and finally 6 DOF coupled models for advanced maneuvers. The models are all expressed in a vectorial setting for effective computer simulation and to simplify control design. Focus is made towards preservation of matrix properties such as symmetry, skew-symmetry, positive definiteness and orthogonality, which are key elements in nonlinear control and estimation theory.

7.1 Maneuvering Models (3 DOF)

The 3 DOF horizontal plane models for maneuvering are based on the rigid-body kinetics:

$$\boldsymbol{M}_{RB}\dot{\boldsymbol{\nu}} + \boldsymbol{C}_{RB}(\boldsymbol{\nu})\boldsymbol{\nu} = \boldsymbol{\tau}_{RB} \tag{7.1}$$

where

$$\boldsymbol{\tau}_{RB} = \boldsymbol{\tau}_{\text{hyd}} + \boldsymbol{\tau}_{\text{hs}} + \boldsymbol{\tau}_{\text{wind}} + \boldsymbol{\tau}_{\text{wave}} + \boldsymbol{\tau} \tag{7.2}$$

The hydrostatic forces $\boldsymbol{\tau}_{\text{hs}} = \mathbf{0}$ in the horizontal plane. From (6.102) under the assumption that $\dot{\boldsymbol{\nu}}_c \approx \mathbf{0}$, it follows that

$$\boldsymbol{\tau}_{\text{hyd}} = -\boldsymbol{M}_A\dot{\boldsymbol{\nu}} - \boldsymbol{C}_A(\boldsymbol{\nu}_r)\boldsymbol{\nu}_r - \boldsymbol{D}(\boldsymbol{\nu}_r)\boldsymbol{\nu}_r \tag{7.3}$$

Combining (7.1), (7.2) and (7.3) gives

Handbook of Marine Craft Hydrodynamics and Motion Control, First Edition. Thor I. Fossen.
 ISBN: 978-1-119-99149-6

$$\dot{\boldsymbol{\eta}} = \boldsymbol{J}_{\Theta}(\boldsymbol{\eta})\boldsymbol{\nu} \tag{7.4}$$

$$\boldsymbol{M}\dot{\boldsymbol{\nu}} + \boldsymbol{C}_{RB}(\boldsymbol{\nu})\boldsymbol{\nu} + \boldsymbol{N}(\boldsymbol{\nu}_r)\boldsymbol{\nu}_r = \boldsymbol{\tau} + \boldsymbol{\tau}_{\text{wind}} + \boldsymbol{\tau}_{\text{wave}} \tag{7.5}$$

where

$$\boldsymbol{N}(\boldsymbol{\nu}_r) := \boldsymbol{C}_A(\boldsymbol{\nu}_r) + \boldsymbol{D}(\boldsymbol{\nu}_r) \tag{7.6}$$

Moreover, added mass Coriolis and centripetal terms together with hydrodynamic damping terms are collected into the matrix $\boldsymbol{N}(\boldsymbol{\nu}_r)$. This is convenient since it is difficult to distinguish terms in $\boldsymbol{C}_A(\boldsymbol{\nu}_r)$ with similar terms in $\boldsymbol{D}(\boldsymbol{\nu}_r)$. Hence, only the sum of these terms is used in the model in order to avoid overparametrization.

In the case of ocean currents it is possible to express (7.5) using only the relative velocity vector $\boldsymbol{\nu}_r$ and thus avoiding terms in $\boldsymbol{\nu}$. In order to do this, $\boldsymbol{C}_{RB}(\boldsymbol{\nu})$ must be parametrized independent of linear velocity, for instance by using (3.57). Hence, it follows from Property 8.1 in Section 8.3 that (7.5) can be rewritten as

$$\boldsymbol{M}\dot{\boldsymbol{\nu}}_r + \underbrace{\boldsymbol{C}(\boldsymbol{\nu}_r)\boldsymbol{\nu}_r + \boldsymbol{D}(\boldsymbol{\nu}_r)\boldsymbol{\nu}_r}_{\boldsymbol{N}(\boldsymbol{\nu}_r)\boldsymbol{\nu}_r} = \boldsymbol{\tau} + \boldsymbol{\tau}_{\text{wind}} + \boldsymbol{\tau}_{\text{wave}} \tag{7.7}$$

where

$$\boldsymbol{M} = \boldsymbol{M}_A + \boldsymbol{M}_{RB} \tag{7.8}$$

$$\boldsymbol{C}(\boldsymbol{\nu}_r) = \boldsymbol{C}_A(\boldsymbol{\nu}_r) + \boldsymbol{C}_{RB}(\boldsymbol{\nu}_r) \tag{7.9}$$

In this representation the generalized velocity $\boldsymbol{\nu}_r$ is the only velocity vector while (7.5) uses both $\boldsymbol{\nu}$ and $\boldsymbol{\nu}_r$.

3 DOF System Matrices

Since the horizontal motion of a ship or semi-submersible is described by the motion components in surge, sway and yaw, the state vectors are chosen as $\boldsymbol{\nu} = [u, v, r]^\top$ and $\boldsymbol{\eta} = [N, E, \psi]^\top$ (see Figure 7.1). This implies that the dynamics associated with the motion in heave, roll and pitch are neglected, that is $w = p = q = 0$. For the horizontal motion of a vessel the kinematic equations of motion reduce from the general 6 DOF expression (2.18) to one principal rotation about the z axis:

$$\boldsymbol{J}_{\boldsymbol{\Theta}}(\boldsymbol{\eta}) \overset{3\,\text{DOF}}{=} \boldsymbol{R}(\psi) = \begin{bmatrix} \cos(\psi) & -\sin(\psi) & 0 \\ \sin(\psi) & \cos(\psi) & 0 \\ 0 & 0 & 1 \end{bmatrix} \tag{7.10}$$

It is also common to assume that the craft has homogeneous mass distribution and xz-plane symmetry such that

$$I_{xy} = I_{yz} = 0 \tag{7.11}$$

Figure 7.1 Displacement vessel where the horizontal plane model can be used for DP and maneuvering.

Let the $\{b\}$-frame coordinate origin be set in the centerline of the craft at the point CO, such that $y_g = 0$. Under the previously stated assumptions, matrices (3.44) and (3.60) associated with the rigid-body kinetics reduce to

$$\boldsymbol{M}_{RB} = \begin{bmatrix} m & 0 & 0 \\ 0 & m & mx_g \\ 0 & mx_g & I_z \end{bmatrix} \tag{7.12}$$

$$\boldsymbol{C}_{RB}(\boldsymbol{\nu}) = \begin{bmatrix} 0 & 0 & -m(x_g r + v) \\ 0 & 0 & mu \\ m(x_g r + v) & -mu & 0 \end{bmatrix} \tag{7.13}$$

Notice that surge is decoupled from sway and yaw in $\boldsymbol{M}_{RB}$ due to symmetry considerations of the system inertia matrix (see Section 3.3). It is assumed that the added mass matrix is computed in CO. This allows for the following reduction of (6.38) and (6.45):

$$\boldsymbol{M}_A = \begin{bmatrix} -X_{\dot{u}} & 0 & 0 \\ 0 & -Y_{\dot{v}} & -Y_{\dot{r}} \\ 0 & -Y_{\dot{r}} & -N_{\dot{r}} \end{bmatrix} \tag{7.14}$$

$$\boldsymbol{C}_A(\boldsymbol{\nu}) = \begin{bmatrix} 0 & 0 & Y_{\dot{v}} v + Y_{\dot{r}} r \\ 0 & 0 & -X_{\dot{u}} u \\ -Y_{\dot{v}} v - Y_{\dot{r}} r & X_{\dot{u}} u & 0 \end{bmatrix} \tag{7.15}$$

where $\boldsymbol{M} = \boldsymbol{M}^\top$, $\boldsymbol{C}_{RB}(\boldsymbol{\nu}) = -\boldsymbol{C}_{RB}^\top(\boldsymbol{\nu})$ and $\boldsymbol{C}_A(\boldsymbol{\nu}) = -\boldsymbol{C}_A(\boldsymbol{\nu})^\top$. Hence,

$$\boldsymbol{M} = \begin{bmatrix} m - X_{\dot{u}} & 0 & 0 \\ 0 & m - Y_{\dot{v}} & mx_g - Y_{\dot{r}} \\ 0 & mx_g - Y_{\dot{r}} & I_z - N_{\dot{r}} \end{bmatrix} \tag{7.16}$$

We will now derive the expressions for $\boldsymbol{N}(\boldsymbol{\nu}_r)$ in (7.6) as a function of $\boldsymbol{C}_A(\boldsymbol{\nu}_r)$ and $\boldsymbol{D}(\boldsymbol{\nu}_r)$.

7.1.1 Nonlinear Maneuvering Models based on Surge Resistance and Cross-Flow Drag

If we use the surge resistance and cross-flow drag models in Section 6.4, the $\boldsymbol{N}(\boldsymbol{\nu}_r)$ matrix in the maneuvering model (7.6) can be expanded as

$$\boldsymbol{N}(\boldsymbol{\nu}_r)\boldsymbol{\nu}_r = \boldsymbol{C}_A(\boldsymbol{\nu}_r)\boldsymbol{\nu}_r + \boldsymbol{D}\boldsymbol{\nu}_r + \boldsymbol{d}(\boldsymbol{\nu}_r) \tag{7.17}$$

where $\boldsymbol{\nu}_r = \boldsymbol{\nu} - \boldsymbol{\nu}_c$ is the relative velocity vector and

$$\boldsymbol{C}_A(\boldsymbol{\nu}_r) = \begin{bmatrix} 0 & 0 & Y_{\dot{v}} v_r + Y_{\dot{r}} r \\ 0 & 0 & -X_{\dot{u}} u_r \\ -Y_{\dot{v}} v_r - Y_{\dot{r}} r & X_{\dot{u}} u_r & 0 \end{bmatrix} \tag{7.18}$$

$$\boldsymbol{D} = \begin{bmatrix} -X_u & 0 & 0 \\ 0 & -Y_v & -Y_r \\ 0 & -N_v & -N_r \end{bmatrix} \tag{7.19}$$

$$\boldsymbol{d}(\boldsymbol{\nu}_r) = \begin{bmatrix} \frac{1}{2}\rho S(1+k) C_f^{\text{new}}(u_r)|u_r|u_r \\ \frac{1}{2}\rho \int_{-L_{pp}/2}^{L_{pp}/2} T(x) C_d^{2D}(x)|v_r + xr|(v_r + xr)\,\mathrm{d}x \\ \frac{1}{2}\rho \int_{-L_{pp}/2}^{L_{pp}/2} T(x) C_d^{2D}(x) x|v_r + xr|(v_r + xr)\,\mathrm{d}x \end{bmatrix} \tag{7.20}$$

The linear damper $\boldsymbol{D}$ in this expression is important for low-speed maneuvering and stationkeeping while the term $\boldsymbol{d}(\boldsymbol{\nu}_r)$ dominates at higher speeds. Linear damping also guarantees that the velocity converges exponentially to zero.

7.1.2 Nonlinear Maneuvering Models based on Second-order Modulus Functions

The idea of using second-order *modulus functions* to describe the nonlinear dissipative terms in $\boldsymbol{N}(\boldsymbol{\nu}_r)$ dates back to Fedyaevsky and Sobolev (1963). Within this framework, a simplified form of Norrbin's nonlinear model (Norrbin, 1970), which retains the most important terms for steering and propulsion

loss assignment, has been proposed by Blanke (1981). This model corresponds to fitting the cross-flow drag integrals (6.91) and (6.92) to second-order modulus functions:[1]

$$\begin{aligned}\boldsymbol{N}(\boldsymbol{\nu}_r)\boldsymbol{\nu}_r &= \boldsymbol{C}_A(\boldsymbol{\nu}_r)\boldsymbol{\nu}_r + \boldsymbol{D}(\boldsymbol{\nu}_r)\boldsymbol{\nu}_r \\ &= \begin{bmatrix} Y_{\dot{v}} v_r r + Y_{\dot{r}} r^2 \\ -X_{\dot{u}} u_r r \\ (X_{\dot{u}} - Y_{\dot{v}}) u_r v_r - Y_{\dot{r}} u_r r \end{bmatrix} \quad \left(\text{alternatively: } \begin{bmatrix} X_{vr} v_r r + X_{rr} r^2 \\ Y_{ur} u_r r \\ N_{uv} u_r v_r + N_{ur} u_r r \end{bmatrix} \right) \\ &\quad + \begin{bmatrix} -X_{|u|u} |u_r| u_r \\ -Y_{|v|v} |v_r| v_r - Y_{|v|r} |v_r| r - Y_{v|r|} v_r |r| - Y_{|r|r} |r| r \\ -N_{|v|v} |v_r| v_r - N_{|v|r} |v_r| r - N_{v|r|} v_r |r| - N_{|r|r} |r| r \end{bmatrix}\end{aligned}$$

or

$$\boldsymbol{N}(\boldsymbol{\nu}_r)\boldsymbol{\nu}_r = \begin{bmatrix} -X_{|u|u} |u_r| u_r + Y_{\dot{v}} v_r r + Y_{\dot{r}} r^2 \\ -X_{\dot{u}} u_r r - Y_{|v|v} |v_r| v_r - Y_{|v|r} |v_r| r - Y_{v|r|} v_r |r| - Y_{|r|r} |r| r \\ (X_{\dot{u}} - Y_{\dot{v}}) u_r v_r - Y_{\dot{r}} u_r r - N_{|v|v} |v_r| v_r - N_{|v|r} |v_r| r - N_{v|r|} v_r |r| - N_{|r|r} |r| r \end{bmatrix} \tag{7.21}$$

From this expression it is seen that

$$\boldsymbol{C}_A(\boldsymbol{\nu}_r) = \begin{bmatrix} 0 & 0 & Y_{\dot{v}} v_r + Y_{\dot{r}} r \\ 0 & 0 & -X_{\dot{u}} u_r \\ -Y_{\dot{v}} v_r - Y_{\dot{r}} r & X_{\dot{u}} u_r & 0 \end{bmatrix} \tag{7.22}$$

$$\boldsymbol{D}(\boldsymbol{\nu}_r) = \begin{bmatrix} -X_{|u|u} |u_r| & 0 & 0 \\ 0 & -Y_{|v|v} |v_r| - Y_{|r|v} |r| & -Y_{|v|r} |v_r| - Y_{|r|r} |r| \\ 0 & -N_{|v|v} |v_r| - N_{|r|v} |r| & -N_{|v|r} |v_r| - N_{|r|r} |r| \end{bmatrix} \tag{7.23}$$

Recall that $\boldsymbol{D}(\boldsymbol{\nu}_r) = \boldsymbol{D} + \boldsymbol{D}_n(\boldsymbol{\nu}_r)$. However, linear potential damping and skin friction $\boldsymbol{D}$ are neglected in (7.21) since the nonlinear quadratic terms $\boldsymbol{D}_n(\boldsymbol{\nu}_r)$ dominate at higher speeds (see Figure 7.2). This is a good assumption for maneuvering while stationkeeping models should include a nonzero $\boldsymbol{D}$.

Figure 7.2 shows the significance of the linear and quadratic terms for different ship speeds. It is recommended to use different damping models depending on the regime of the control system. In many cases, it is important to include both linear and quadratic damping, since only quadratic damping in the model will cause oscillatory behavior at low speed. The main reason is that linear damping is needed for exponential convergence to zero. For marine craft operating in waves, linear damping will always be present due to potential damping and linear skin friction (Faltinsen and Sortland, 1987). For large ships Blanke (1981) suggests simplifying (7.23) according to

$$\boldsymbol{D}_n(\boldsymbol{\nu}_r) = \begin{bmatrix} -X_{|u|u} |u_r| & 0 & 0 \\ 0 & -Y_{|v|v} |v_r| & -Y_{|v|r} |v_r| \\ 0 & -N_{|v|v} |v_r| & -N_{|v|r} |v_r| \end{bmatrix} \tag{7.24}$$

[1] The $\boldsymbol{C}_A$ terms can also be denoted as $X_{vr} v_r r$, $X_{rr} r^2$, $Y_{ur} u_r r$, $N_{uv} u_r v_r$ and $N_{ur} u_r r$. If these terms are experimentally obtained, viscous effects will be included in addition to the potential coefficients $Y_{\dot{v}}$, $X_{\dot{u}}$ and $Y_{\dot{r}}$.

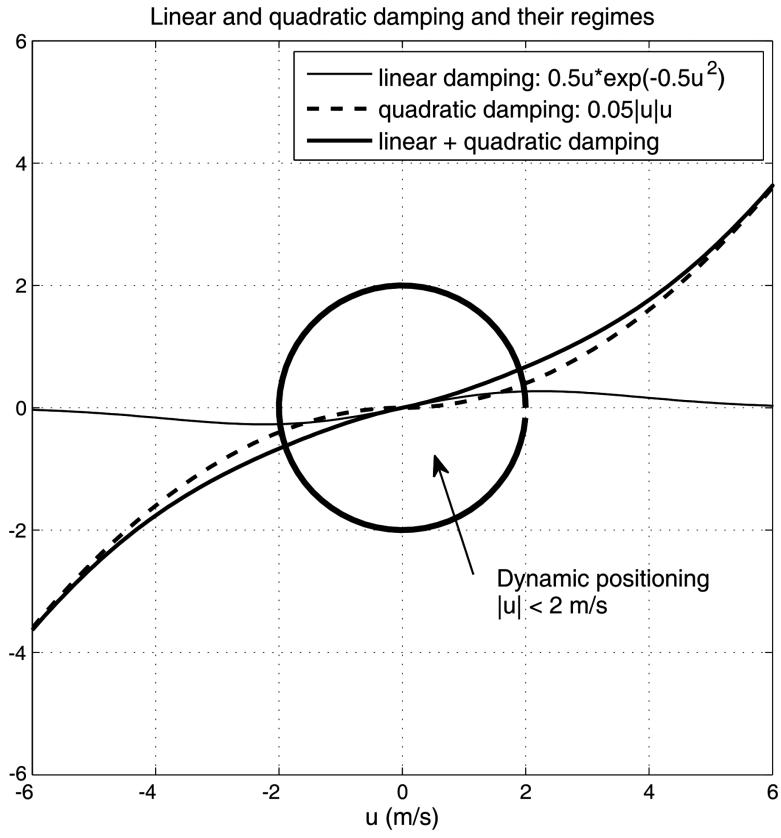

Figure 7.2 Linear and quadratic damping and their speeds regimes. Notice that the linear part goes to zero for higher speeds.

This gives

$$\boldsymbol{N}(\boldsymbol{\nu}_r) = \boldsymbol{C}_A(\boldsymbol{\nu}_r) + \boldsymbol{D}(\boldsymbol{\nu}_r) \tag{7.25}$$
$$= \begin{bmatrix} -X_{|u|u}\,|u_r| & 0 & Y_{\dot{v}}v_r + Y_{\dot{r}}r \\ 0 & -Y_{|v|v}\,|v_r| & -X_{\dot{u}}u_r - Y_{|v|r}\,|v_r| \\ -Y_{\dot{v}}v_r - Y_{\dot{r}}r & X_{\dot{u}}u_r - N_{|v|v}\,|v_r| & -N_{|v|r}\,|v_r| \end{bmatrix}$$

7.1.3 Nonlinear Maneuvering Models based on Odd Functions

So far, we have discussed nonlinear maneuvering models based on first principles such as surge resistance and cross-flow drag, which have been approximated by second-order *modulus functions* (see Fedyaevsky and Sobolev, 1963; Norrbin, 1970). In many cases a more pragmatic approach is used for curve fitting of experimental data (Clarke, 2003). This is typically done by using *Taylor series* of first- and second-order terms (Abkowitz, 1964) to describe the nonlinear terms in $\boldsymbol{N}(\boldsymbol{\nu}_r)$.

The Nonlinear Model of Abkowitz (1964)

One of the standard nonlinear ship models in the literature is that of Abkowitz (1964). Consider the nonlinear rigid-body kinetics:

$$\boldsymbol{M}_{RB}\dot{\boldsymbol{\nu}} + \boldsymbol{C}_{RB}(\boldsymbol{\nu})\boldsymbol{\nu} = \boldsymbol{\tau}_{RB} \tag{7.26}$$

with external forces and moment:

$$\boldsymbol{\tau}_{RB} = [X(\boldsymbol{x}),\, Y(\boldsymbol{x}),\, N(\boldsymbol{x})]^\top \tag{7.27}$$

where

$$\boldsymbol{x} = [u,\, v,\, r,\, \dot{u},\, \dot{v},\, \dot{r},\, \delta]^\top \tag{7.28}$$

and δ is the rudder angle. Based on these equations, Abkowitz (1964) proposed a third-order truncated *Taylor-series* expansion of the functions $X(\boldsymbol{x})$, $Y(\boldsymbol{x})$ and $N(\boldsymbol{x})$ at

$$\boldsymbol{x}_o = [U,\, 0,\, 0,\, 0,\, 0,\, 0,\, 0]^\top \tag{7.29}$$

This gives

$$X(\boldsymbol{x}) \approx X(\boldsymbol{x}_0) + \sum_{i=1}^{n} \left(\frac{\partial X(\boldsymbol{x})}{\partial x_i}\bigg|_{\boldsymbol{x}_0} \Delta x_i + \frac{1}{2}\,\frac{\partial^2 X(\boldsymbol{x})}{(\partial x_i)^2}\bigg|_{\boldsymbol{x}_0} \Delta x_i^2 + \frac{1}{6}\,\frac{\partial^3 X(\boldsymbol{x})}{(\partial x_i)^3}\bigg|_{\boldsymbol{x}_0} \Delta x_i^3 \right)$$

$$Y(\boldsymbol{x}) \approx Y(\boldsymbol{x}_0) + \sum_{i=1}^{n} \left(\frac{\partial Y(\boldsymbol{x})}{\partial x_i}\bigg|_{\boldsymbol{x}_0} \Delta x_i + \frac{1}{2}\,\frac{\partial^2 Y(\boldsymbol{x})}{(\partial x_i)^2}\bigg|_{\boldsymbol{x}_0} \Delta x_i^2 + \frac{1}{6}\,\frac{\partial^3 Y(\boldsymbol{x})}{(\partial x_i)^3}\bigg|_{\boldsymbol{x}_0} \Delta x_i^3 \right)$$

$$N(\boldsymbol{x}) \approx Z(\boldsymbol{x}_0) + \sum_{i=1}^{n} \left(\frac{\partial N(\boldsymbol{x})}{\partial x_i}\bigg|_{\boldsymbol{x}_0} \Delta x_i + \frac{1}{2}\,\frac{\partial^2 N(\boldsymbol{x})}{(\partial x_i)^2}\bigg|_{\boldsymbol{x}_0} \Delta x_i^2 + \frac{1}{6}\,\frac{\partial^3 N(\boldsymbol{x})}{(\partial x_i)^3}\bigg|_{\boldsymbol{x}_0} \Delta x_i^3 \right)$$

where $\Delta\boldsymbol{x} = \boldsymbol{x} - \boldsymbol{x}_0 = [\Delta x_1, \Delta x_2, \ldots, \Delta x_7]^\top$. Unfortunately, a third-order Taylor-series expansion results in a large number of terms. By applying some physical insight, the complexity of these expressions can be reduced. Abkowitz (1964) makes the following assumptions:

1. *Most ship maneuvers can be described by a 3rd-order truncated Taylor expansion about the steady state condition $u = u_0$.*
2. *Only 1st-order acceleration terms are considered.*
3. *Standard port/starboard symmetry simplifications except terms describing the constant force and moment arising from single-screw propellers.*
4. *The coupling between the acceleration and velocity terms is negligible.*

Simulations of standard ship maneuvers show that these assumptions are quite good. Applying these assumptions to the expressions $X(\boldsymbol{x})$, $Y(\boldsymbol{x})$ and $N(\boldsymbol{x})$ yields

$$\begin{aligned} X = {} & X^* + X_{\dot{u}}\dot{u} + X_u\Delta u + X_{uu}\Delta u^2 + X_{uuu}\Delta u^3 + X_{vv}v^2 + X_{rr}r^2 + X_{\delta\delta}\delta^2 \\ & + X_{rv\delta}rv\delta + X_{r\delta}r\delta + X_{v\delta}v\delta + X_{vvu}v^2\Delta u + X_{rru}r^2\Delta u + X_{\delta\delta u}\delta^2\Delta u \\ & + X_{rvu}rvu + X_{r\delta u}r\delta\Delta u + X_{v\delta u}v\delta\Delta u \end{aligned}$$

$$
\begin{aligned}
Y &= Y^* + Y_u\Delta u + Y_{uu}\Delta u^2 + Y_r r + Y_v v + Y_{\dot r}\dot r + Y_{\dot v}\dot v + Y_\delta \delta + Y_{rrr} r^3 + Y_{vvv} v^3 \\
&\quad + Y_{\delta\delta\delta}\delta^3 + Y_{rr\delta} r^2\delta + Y_{\delta\delta r}\delta^2 r + Y_{rrv} r^2 v + Y_{vvr} v^2 r + Y_{\delta\delta v}\delta^2 v + Y_{vv\delta} v^2\delta + Y_{\delta vr}\delta v r \\
&\quad + Y_{vu} v\Delta u + Y_{vuu} v\Delta u^2 + Y_{ru} r\Delta u + Y_{ruu} r\Delta u^2 + Y_{\delta u}\delta\Delta u + Y_{\delta uu}\delta\Delta u^2 \\
N &= N^* + N_u\Delta u + N_{uu}\Delta u^2 + N_r r + N_v v + N_{\dot r}\dot r + N_{\dot v}\dot v + N_\delta \delta + N_{rrr} r^3 + N_{vvv} v^3 \\
&\quad + N_{\delta\delta\delta}\delta^3 + N_{rr\delta} r^2\delta + N_{\delta\delta r}\delta^2 r + N_{rrv} r^2 v + N_{vvr} v^2 r + N_{\delta\delta v}\delta^2 v + N_{vv\delta} v^2\delta \\
&\quad + N_{\delta vr}\delta v r + N_{vu} v\Delta u + N_{vuu} v\Delta u^2 + N_{ru} r\Delta u + N_{ruu} r\Delta u^2 + N_{\delta u}\delta\Delta u \\
&\quad + N_{\delta uu}\delta\Delta u^2
\end{aligned}
\tag{7.30}
$$

The hydrodynamic derivatives (7.30) are defined using the notation

$$
F^* = F(\boldsymbol{x}_0), \quad F_{x_i} = \left.\frac{\partial F(\boldsymbol{x})}{\partial x_i}\right|_{\boldsymbol{x}_0}
$$

$$
F_{x_i x_j} = \frac{1}{2}\left.\frac{\partial^2 F(\boldsymbol{x})}{\partial x_i \partial x_j}\right|_{\boldsymbol{x}_0}, \quad F_{x_i x_j x_k} = \frac{1}{6}\left.\frac{\partial^3 F(\boldsymbol{x})}{\partial x_i \partial x_j \partial x_k}\right|_{\boldsymbol{x}_0}
$$

where $F \in \{X, Y, N\}$.

PMM Models

The hydrodynamic coefficients can be experimentally determined by using a planar-motion-mechanism (PMM) system, which is a device for experimentally determining the hydrodynamic derivatives required in the equations of motion. This includes coefficients usually classified into the three categories of static stability, rotary stability and acceleration derivatives. The PMM device is capable of oscillating a ship (or submarine) model while it is being towed in a testing tank. The forces are measured on the scale model and fitted to odd functions based on Taylor-series expansions. The resulting model is usually referred to as the PMM model and this model is scaled up to a full-scale ship by using Froude number similarity. This ensures that the ratio between the inertial and gravitational forces is kept constant.

7.1.4 Linearized Maneuvering Models

For marine craft moving at constant (or at least slowly varying) forward speed,

$$
U = \sqrt{u^2 + v^2} \approx u \tag{7.31}
$$

The 3 DOF maneuvering model of Section 7.1.1 can be decoupled in a forward speed (surge) model and a sway–yaw subsystem for maneuvering.

Forward Speed Model (Surge Subsystem)

Starboard–port symmetry implies that surge is decoupled from sway and yaw. Hence, the surge equation in Section 7.1.1 can be written in component form as

$$(m - X_{\dot{u}})\dot{u} - X_u u_r - X_{|u|u}\,|u_r|\,u_r = \tau_1 \tag{7.32}$$

where τ_1 is the sum of control and external forces in surge.

Linearized Maneuvering Model (Sway–Yaw Subsystem)

The linearized maneuvering model known as the *potential theory representation* can be written (Fossen, 1994, Clarke and Horn, 1997)

$$\boldsymbol{M}\dot{\boldsymbol{v}} + \boldsymbol{N}(u_o)\boldsymbol{v}_r = \boldsymbol{b}\delta \tag{7.33}$$

where $\boldsymbol{v}_r = [v_r, r]^\top$ and δ is the rudder angle. This is based on the assumptions that the cruise speed

$$u = u_o \approx \text{constant} \tag{7.34}$$

and that v_r and r are small. The ocean current force is included as a linear term $\boldsymbol{N}(u_o)[v_c, 0]^\top$. The potential theory representation is obtained by extracting the 2nd and 6th rows in $\boldsymbol{C}_{RB}(\boldsymbol{v})$ and $\boldsymbol{C}_A(\boldsymbol{v})$, Equations (3.60) and (6.45), with $u = u_o$, resulting in

$$\begin{aligned}\boldsymbol{C}(\boldsymbol{v})\boldsymbol{v} &\approx \begin{bmatrix} (m - X_{\dot{u}})u_o r \\ (m - Y_{\dot{v}})u_o v + (mx_g - Y_{\dot{r}})u_o r - (m - X_{\dot{u}})u_o v \end{bmatrix} \\ &= \begin{bmatrix} 0 & (m - X_{\dot{u}})u_o \\ (X_{\dot{u}} - Y_{\dot{v}})u_o & (mx_g - Y_{\dot{r}})u_o \end{bmatrix} \begin{bmatrix} v \\ r \end{bmatrix}\end{aligned} \tag{7.35}$$

Linear damping in sway and yaw takes the following form:

$$\boldsymbol{D} = \begin{bmatrix} -Y_v & -Y_r \\ -N_v & -N_r \end{bmatrix} \tag{7.36}$$

Assuming that the ship is controlled by a single rudder:

$$\begin{aligned}\boldsymbol{\tau} &= \boldsymbol{b}\delta \\ &= \begin{bmatrix} -Y_\delta \\ -N_\delta \end{bmatrix} \delta\end{aligned} \tag{7.37}$$

and that $\boldsymbol{N}(u_o)$ contains the speed-dependent terms from $\boldsymbol{C}(\boldsymbol{v})$ and the linear damper $\boldsymbol{D}$, finally gives

$$\boldsymbol{M} = \begin{bmatrix} m - Y_{\dot{v}} & mx_g - Y_{\dot{r}} \\ mx_g - Y_{\dot{r}} & I_z - N_{\dot{r}} \end{bmatrix} \tag{7.38}$$

$$\boldsymbol{N}(u_o) = \begin{bmatrix} -Y_v & (m - X_{\dot{u}})u_o - Y_r \\ (X_{\dot{u}} - Y_{\dot{v}})u_o - N_v & (mx_g - Y_{\dot{r}})u_o - N_r \end{bmatrix} \tag{7.39}$$

$$\boldsymbol{b} = \begin{bmatrix} -Y_\delta \\ -N_\delta \end{bmatrix} \tag{7.40}$$

Comment 7.1
Davidson and Schiff (1946) assumed that the hydrodynamic forces $\boldsymbol{\tau}_{RB}$ are linear in δ, $\dot{\boldsymbol{\nu}}$ and $\boldsymbol{\nu}$ (linear strip theory) such that

$$\boldsymbol{\tau}_{RB} = -\underbrace{\begin{bmatrix} Y_\delta \\ N_\delta \end{bmatrix}}_{\boldsymbol{b}} \delta + \underbrace{\begin{bmatrix} Y_{\dot{v}} & Y_{\dot{r}} \\ N_{\dot{v}} & N_{\dot{r}} \end{bmatrix}}_{\boldsymbol{M}_A} \dot{\boldsymbol{\nu}} + \underbrace{\begin{bmatrix} Y_v & Y_r \\ N_v & N_r \end{bmatrix}}_{\boldsymbol{D}} \boldsymbol{\nu}_r \tag{7.41}$$

This gives

$$\boldsymbol{N}(u_o) = \begin{bmatrix} -Y_v & mu_o - Y_r \\ -N_v & mx_g u_o - N_r \end{bmatrix} \tag{7.42}$$

Notice that the Munk moment $(X_{\dot{u}} - Y_{\dot{v}})u_o v$ is missing in the yaw equation when compared to (7.39). This is a destabilizing moment known from aerodynamics which tries to turn the craft; see Faltinsen (1990, pp. 188–189). Also notice that the less important terms $X_{\dot{u}}u_o r$ and $Y_{\dot{r}}u_o r$ are removed from $\boldsymbol{N}$ when compared to (7.39). All missing terms terms are due to the $\boldsymbol{C}_A(\boldsymbol{\nu})$ matrix, which is omitted in the linear expression (7.41). Consequently, it is recommended to use (7.39), which includes the terms from the $\boldsymbol{C}_A(\boldsymbol{\nu}_r)$ matrix.

Hydrodynamic Derivatives

The hydrodynamic derivatives in (7.38) and (7.39) are related to the zero-speed potential coefficients according to

$$\begin{aligned} -Y_{\dot{v}} &= A_{22}(0) & -N_{\dot{v}} &= A_{62}(0) \\ -Y_{\dot{r}} &= A_{26}(0) & -N_{\dot{r}} &= A_{66}(0) \\ \\ -Y_v &= B_{22}(0) + B_{22v} & -N_v &= B_{62}(0) + B_{62v} \\ -Y_r &= B_{26}(0) + B_{26v} & -N_r &= B_{66}(0) + B_{66v} \end{aligned} \tag{7.43}$$

where the subscript v for the B elements denotes the viscous contribution.

7.2 Autopilot Models for Heading Control (1 DOF)

Model-based heading controllers for marine craft are usually based on the model representation of Nomoto *et al.* (1957).The Nomoto autopilot model can be derived from the linearized maneuvering model, as explained below.

7.2.1 Second-Order Nomoto Model (Yaw Subsystem)

A linear autopilot model for heading control can be derived from the maneuvering model

$$\boldsymbol{M}\dot{\boldsymbol{\nu}} + \boldsymbol{N}(u_o)\boldsymbol{\nu} = \boldsymbol{b}\delta \tag{7.44}$$

by choosing the yaw rate r as output:

$$r = \boldsymbol{c}^\top \boldsymbol{v}, \quad \boldsymbol{c}^\top = [0, 1] \tag{7.45}$$

Hence, application of the *Laplace transformation* yields

$$\frac{r}{\delta}(s) = \frac{K(1 + T_3 s)}{(1 + T_1 s)(1 + T_2 s)} \tag{7.46}$$

A similar expression is obtained for the sway motion:

$$\frac{v}{\delta}(s) = \frac{K_v(1 + T_v s)}{(1 + T_1 s)(1 + T_2 s)} \tag{7.47}$$

where K_v and T_v differ from K and T_3 in the yaw equation.

Equation (7.46) is referred to as *Nomoto's second-order model* (Nomoto *et al.*, 1957).

7.2.2 First-Order Nomoto Model (Yaw Subsystem)

The *first-order Nomoto model* is obtained by defining the *equivalent time constant:*

$$T := T_1 + T_2 - T_3 \tag{7.48}$$

such that

$$\frac{r}{\delta}(s) = \frac{K}{(1 + Ts)} \tag{7.49}$$

Finally, $\dot{\psi} = r$ yields

$$\frac{\psi}{\delta}(s) = \frac{K}{s(1 + Ts)} \tag{7.50}$$

which is the transfer function that is used in most commercial autopilot systems.

Time-Domain Representations of the First- and Second-Order Nomoto Models

The time-domain representation for Nomoto's second-order model becomes

$$T_1 T_2 \psi^{(3)} + (T_1 + T_2)\ddot{\psi} + \dot{\psi} = K(\delta + T_3 \dot{\delta}) \tag{7.51}$$

which can be approximated by

$$T\ddot{\psi} + \dot{\psi} = K\delta \tag{7.52}$$

The accuracy of the first-order Nomoto model when compared to the second-order model is illustrated in Example 7.1 where a course stable cargo ship and a course unstable oil tanker are considered (see Section 12.1.1).

Matlab

```
function nomoto(T1,T2,T3,K)
% NOMOTO(T1,T2,T3,K) generates the Bode plots for
%
%            K                    K (1+T3s)
% H1(s) = ------      H2(s) = ----------------
%         (1+Ts)s              s(1+T1s)(1+T2s)
%
% Author:    Thor I. Fossen

T = T1+T2-T3;
d1 = [T 1 0];               n1 = K;
d2 = [T1*T2 T1+T2 1 0];     n2 = K*[T3 1];
[mag1,phase1,w] = bode(n1,d1);
[mag2,phase2]    = bode(n2,d2,w);

% shift ship phase with 360 deg for course unstable ship
if K < 0,
phase1 = phase1-360;
phase2 = phase2-360;
end

clf,subplot(211),semilogx(w,20*log10(mag1)),grid
xlabel('Frequency [rad/s]'),title('Gain [dB]')
hold on,semilogx(w,20*log10(mag2),'-'),hold off
subplot(212),semilogx(w,phase1),grid
xlabel('Frequency [rad/s]'),title('Phase [deg]')
hold on,semilogx(w,phase2,'-'),hold off
```

Example 7.1 (Frequency Response for Nomoto First- and Second-Order Models)
Consider a Mariner class cargo ship (Chislett and Strøm-Tejsen, 1965a) and a fully loaded tanker (Dyne and Trägårdh, 1975) given by the parameters in Table 7.1. The Bode diagram is generated by using the MSS toolbox commands:

```
T1=118; T2=7.8; T3=18.5; K=0.185;
nomoto(T1, T2, T3, K)

T1=-124.1; T2=16.4; T3=46.0; K=-0.019;
nomoto(T1, T2, T3, K)
```

It is seen from Figure 7.3 that the first-order approximation is quite accurate up to 0.1 rad/s *for the cargo ship and the tanker. A small deviation in the phase around* 0.5 rad/s *is observed. This is due to the cancelation of the sway dynamics.*

Table 7.1 Parameters for a cargo ship and a fully loaded oil tanker

	L(m)	u_0(m/s)	∇(dwt)	K(1/s)	T_1(s)	T_2(s)	T_3(s)
Cargo ship	161	7.7	16622	0.185	118.0	7.8	18.5
Oil tanker	350	8.1	389100	−0.019	−124.1	16.4	46.0

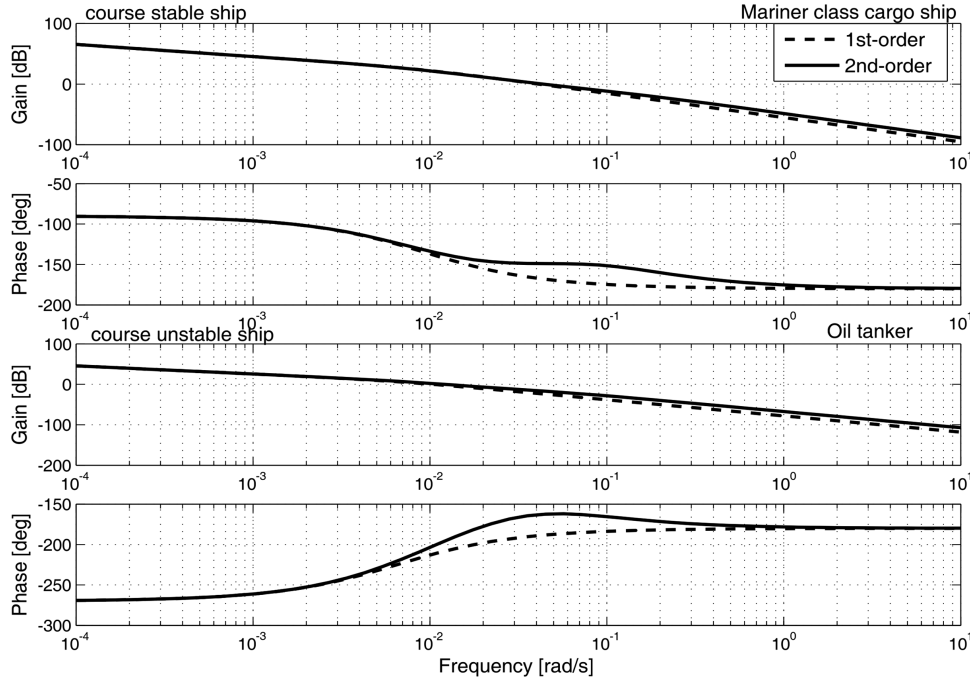

Figure 7.3 First-order and second-order Nomoto transfer functions for a course-stable Mariner class cargo ship and a course-unstable oil tanker.

7.2.3 Nonlinear Extensions of Nomoto's Model

The linear Nomoto model can be extended to include nonlinear effects by adding a *static nonlinearity* to describe the *maneuvering characteristics*.

Nonlinear Extension of Nomoto's First-Order Model

In Norrbin (1963) the following first-order model was proposed:

$$T\dot{r} + H_N(r) = K\delta \tag{7.53}$$

$$H_N(r) = n_3 r^3 + n_2 r^2 + n_1 r + n_0 \tag{7.54}$$

where $H_N(r)$ is a nonlinear function. For $H_N(r) = r$, the linear model (7.52) is obtained.

Nonlinear Extension of Nomoto's Second-Order Model

Bech and Wagner Smith (1969) propose a second-order model:

$$T_1 T_2 \ddot{r} + (T_1 + T_2)\dot{r} + K H_B(r) = K(\delta + T_3 \dot{\delta}) \tag{7.55}$$

$$H_B(r) = b_3 r^3 + b_2 r^2 + b_1 r + b_0 \tag{7.56}$$

where $H_B(r)$ can be found from Bech's reverse spiral maneuver. The linear equivalent (7.51) is obtained for $H_B(r) = r$.

The linear and nonlinear maneuvering characteristics are shown in Figure 12.12 in Section 12.1.2. They are generated by solving for r as a function of δ using the steady-state solutions of (7.53) or (7.55):

$$H_N(r) = K\delta, \quad H_B(r) = \delta \tag{7.57}$$

The nonlinear maneuvering characteristics can also be generated from full-scale maneuvering tests. For stable ships both the *Bech* and *Dieudonne spiral tests* can be applied, while the Bech spiral is the only one avoiding the hysteresis effect for course-unstable ships; see Section 12.1.2 for details.

For a course-unstable ship, $b_1 < 0$, whereas a course-stable ship satisfies $b_1 > 0$. A single-screw propeller or asymmetry in the hull will cause a nonzero value of b_0. Similarly, symmetry in the hull implies that $b_2 = 0$. Since a constant rudder angle is required to compensate for constant steady-state wind and current forces, the bias term b_0 could conveniently be treated as an additional rudder off set. This in turn implies that a large number of ships can be described by the polynomial

$$H_B(r) = b_3 r^3 + b_1 r \tag{7.58}$$

The coefficients b_i $(i = 0, \ldots, 3)$ are related to those in Norrbin's model n_i $(i = 0, \ldots, 3)$ by

$$n_i = \frac{b_i}{|b_1|} \tag{7.59}$$

resulting in

$$H_N(r) = n_3 r^3 + n_1 r \tag{7.60}$$

This implies that $n_1 = 1$ for a course-stable ship and $n_1 = -1$ for a course-unstable ship.

7.2.4 Pivot Point (Yaw Rotation Point)

When turning a ship it is important to know at which point the ship turns about. This rotation point or *pivot point* in yaw is defined as follows:

Definition 7.1 (Pivot Point)
A ship's pivot point x_p is a point on the centerline measured from the CG about which the ship turns. Consequently, it has no sideways movement (Tzeng, 1998a):

$$v_{p/n} = v_{g/n} + x_p r \equiv 0 \tag{7.61}$$

and $v_{g/n}$ is the sway velocity of CG with respect to $\{n\}$. The pivot point will scribe the ship's turning circle.

It is possible to compute the pivot point for a turning ship online by measuring the velocity $v_{g/n}(t)$ in the CG and the turning rate $r(t)$. From (7.61) it follows that

$$x_p(t) = -\frac{v_{g/n}(t)}{r(t)}, \quad r(t) \neq 0 \tag{7.62}$$

This expression is not defined for a zero yaw rate corresponding to a straight-line motion. This means that the pivot point is located at infinity when moving on a straight line or in a pure sway motion.

It is well known to the pilots that the pivot point of a turning ship is located at about 1/5 to 1/4 ship length aft of bow (Tzeng, 1998a). The location of the pivot point of a rudder controlled ship is related to the ratio of the *sway-rudder* and *yaw-rudder* gain coefficients. This can be explained by considering the linearized maneuvering equations in the steady state. From (7.46) and (7.47) we have

$$\begin{aligned} \frac{v}{r} &= \frac{K_v(1 + T_v s)}{K(1 + T_3 s)} \\ &\overset{s=0}{=} \frac{K_v}{K} \end{aligned} \tag{7.63}$$

Consequently, the steady-state location of the pivot point is given by

$$x_{p(s,s)} = -\frac{K_v}{K} \tag{7.64}$$

This expression can also be related to the hydrodynamic derivatives according to

$$x_{p(s,s)} = -\frac{N_r Y_\delta - (Y_r - mu_0)N_\delta}{Y_v N_\delta - N_v Y_\delta} \tag{7.65}$$

Notice that $x_{p(s,s)}$ depends on the forward speed u_0. The nondimensional form becomes (see Section 7.2.5)

$$\begin{aligned} x'_{p(s,s)} &= \frac{x_{p(s,s)}}{L_{pp}} \\ &= -\frac{N'_r Y'_\delta - (Y'_r - m'u'_0)N'_\delta}{Y'_v N'_\delta - N'_v Y'_\delta} \end{aligned} \tag{7.66}$$

Example 7.2 (Pivot Point for the Mariner Class Vessel)
Consider the Mariner Class vessel (Chislett and Strøm-Tejsen, 1965b) where the nondimensional linear maneuvering coefficients for $u_0 = 7.175$ m/s (15 knots) are given as

$$\begin{aligned} Y'_v &= -1160 \times 10^{-5} & N'_v &= -264 \times 10^{-5} \\ Y'_r - m'u'_0 &= -499 \times 10^{-5} & N'_r &= -166 \times 10^{-5} \\ Y'_\delta &= 278 \times 10^{-5} & N'_\delta &= -139 \times 10^{-5} \end{aligned}$$

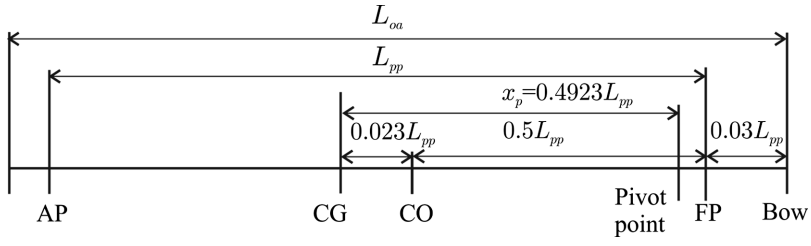

Figure 7.4 Location of the pivot point for the Mariner Class vessel.

The Mariner Class vessel is programmed in the MSS toolbox file mariner.m. The nondimensional pivot point is computed from (7.66). This gives

$$x'_{p(s,s)} = 0.4923 \tag{7.67}$$

or

$$x_{p(s,s)} = 0.4923 L_{pp} \tag{7.68}$$

where $L_{pp} = 160.93$ m *is the length between the perpendiculars AP and FP. The overall length is* $L_{oa} = 171.8$ m. *The pivot point* $x_{p(s,s)}$ *is located ahead of the CG. Since the CG is located at* $x_g = -0.023 L_{pp}$ *and the bow is approximately* $0.03 L_{pp}$ *fore of FP, the pivot point is* $0.06 L_{pp}$ *aft of the bow (see Figure 7.4).*

7.2.5 Nondimensional Maneuvering and Autopilot Models

When designing course autopilots it is often convenient to normalize the ship steering equations of motion such that the model parameters can be treated as constants with respect to the instantaneous speed U defined by

$$U = \sqrt{u^2 + v^2} = \sqrt{(u_0 + \Delta u)^2 + \Delta v^2} \tag{7.69}$$

where u_0 is the *service speed* and Δu and Δv are small perturbations in the surge and sway velocities, respectively. Hence,

$$U \approx u_0 \tag{7.70}$$

During course-changing maneuvers the instantaneous speed will decrease due to increased resistance during the turn.

The most commonly used normalization forms for marine craft are the *prime system* of SNAME (1950) and the *bis system* of Norrbin (1970).

Prime System: This system uses the craft's instantaneous speed U, the length $L = L_{pp}$ (the length between the fore and aft perpendiculars), the time unit L/U and the mass unit $1/2\rho L^3$ or $1/2\rho L^2 T$ as normalization variables. The latter is inspired by wing theory, where the reference area $A = LT$ is used instead of $A = L^2$. The prime system cannot be used for low-speed applications such as dynamic ship positioning, since normalization of the velocities u, v and w implies dividing by the cruise speed U, which can be zero for a dynamically positioned ship. As a consequence, the prime system is mostly used in ship maneuvering.

Bis System: This system can be used for zero-speed as well as high-speed applications since division of speed U is avoided. The bis system is based on the use of the length $L = L_{pp}$, with the time unit

Table 7.2 Normalization variables used for the prime and bis systems

Unit	Prime system I	Prime system II	Bis system
Length	L	L	L
Mass	$\frac{1}{2}\rho L^3$	$\frac{1}{2}\rho L^2 T$	$\mu\rho\nabla$
Inertia moment	$\frac{1}{2}\rho L^5$	$\frac{1}{2}\rho L^4 T$	$\mu\rho\nabla L^2$
Time	$\frac{L}{U}$	$\frac{L}{U}$	$\sqrt{L/g}$
Reference area	L^2	LT	$\mu\ \frac{2\nabla}{L}$
Position	L	L	L
Angle	1	1	1
Linear velocity	U	U	$\sqrt{Lg}$
Angular velocity	$\frac{U}{L}$	$\frac{U}{L}$	$\sqrt{g/L}$
Linear acceleration	$\frac{U^2}{L}$	$\frac{U^2}{L}$	g
Angular acceleration	$\frac{U^2}{L^2}$	$\frac{U^2}{L^2}$	$\frac{g}{L}$
Force	$\frac{1}{2}\rho U^2 L^2$	$\frac{1}{2}\rho U^2 LT$	$\mu\rho g\nabla$
Moment	$\frac{1}{2}\rho U^2 L^3$	$\frac{1}{2}\rho U^2 L^2 T$	$\mu\rho g\nabla L$

$\sqrt{L/g}$ such that speed becomes $\sqrt{Lg} > 0$. In addition, the body mass density ratio $\mu = m/\rho\nabla$, where m is the mass unit and ∇ is the hull contour displacement, is applied. The density ratio μ takes the following values:

$\mu < 1$	Underwater vehicles (ROVs, AUVs and submarines)
$\mu = 1$	Floating ships/rigs and neutrally buoyant underwater vehicles
$\mu > 1$	Heavy torpedoes (typically $\mu = 1.3$–1.5)

The normalization variables for the prime and bis systems are given in Table 7.2. The nondimensional quantities will be distinguished from those with dimension by applying the notation $(\cdot)'$ for the prime system and $(\cdot)''$ for the bis system.

Example 7.3 (Normalization of Parameters)
The hydrodynamic coefficient Y_r can be made nondimensional by using the prime and bis systems. First, let us determine the dimension of Y_r. Consider

$$\underbrace{Y}_{[N=kgm/s^2]} = \underbrace{Y_r}_{[\text{unknown}]}\ \underbrace{r}_{[\text{rad/s}]}$$

Hence, the unknown dimension must be kg m/s since rad *is a nondimensional unit. The nondimensional values Y_r' and Y_r'' are found by using kg, m and s from Table 7.2. Consequently,*

$$Y_r' = \frac{Y_r}{\frac{\left[\frac{1}{2}\rho L^3\right][L]}{[L/U]}} = \frac{1}{\frac{1}{2}\rho L^3 U} Y_r \tag{7.71}$$

$$Y_r'' = \frac{Y_r}{\frac{[\mu\rho\nabla][L]}{\sqrt{L/g}}} = \frac{1}{\mu\rho\nabla\sqrt{Lg}} Y_r \tag{7.72}$$

For a floating ship, Y_r'' can be further simplified since $\mu = 1$ and $m = \rho\nabla$. Hence,

$$Y_r'' = \frac{1}{m\sqrt{Lg}} Y_r \tag{7.73}$$

Example 7.4 (Normalization of States and Parameters)
Consider the linear maneuvering model (7.33). Normalization according to the prime system suggests

$$\boldsymbol{M}'\dot{\boldsymbol{\nu}}' + \boldsymbol{N}'(u_0')\boldsymbol{\nu}' = \boldsymbol{b}'\delta' \tag{7.74}$$

where $\boldsymbol{\nu}' = [v', r']^\top$ *and*

$$\boldsymbol{M}' = \begin{bmatrix} m' - Y_{\dot{v}}' & m'x_g' - Y_{\dot{r}}' \\ m'x_g' - N_{\dot{v}}' & I_z' - N_{\dot{r}}' \end{bmatrix}, \quad \boldsymbol{b}' = \begin{bmatrix} -Y_\delta' \\ -N_\delta' \end{bmatrix}, \quad \boldsymbol{N}'(u_0') = \begin{bmatrix} -Y_v' & m'u_0' - Y_r' \\ -N_v' & m'x_g'u_0' - N_r' \end{bmatrix}$$

where

$$u_0' = \frac{u_0}{U} \approx 1, \quad \textit{for } \Delta u \approx 0 \textit{ and } \Delta v \approx 0 \tag{7.75}$$

The nondimensional velocities and control input can be transformed to its dimensional values by

$$v = Uv', \quad r = \frac{U}{L}r', \quad \delta = \delta' \tag{7.76}$$

6 DOF Normalization Procedure

A systematic procedure for 6 DOF normalization is found by defining a transformation matrix:

$$\boldsymbol{T} = \text{diag}\left\{1, 1, 1, \frac{1}{L}, \frac{1}{L}, \frac{1}{L}\right\} \tag{7.77}$$

$$\boldsymbol{T}^{-1} = \text{diag}\{1, 1, 1, L, L, L\} \tag{7.78}$$

Consider the nondimensional MIMO model (see Example 7.4)

$$\boldsymbol{M}'\dot{\boldsymbol{\nu}}' + \boldsymbol{N}'\boldsymbol{\nu}' + \boldsymbol{G}'\boldsymbol{\eta}' = \boldsymbol{\tau}' \tag{7.79}$$

When designing marine craft simulators and gain-scheduled controllers it is convenient to perform the numerical integration in real time using dimensional time. Consequently, it is convenient to use the nondimensional hydrodynamic coefficients as input to the simulator or controller, while the states $\boldsymbol{\nu}$, $\boldsymbol{\eta}$ and input $\boldsymbol{\tau}$ should have their physical dimensions. For the *prime system* this is obtained by applying the following transformation to (7.79):

$$\boldsymbol{M}'\left(\frac{L}{U^2}\boldsymbol{T}^{-1}\dot{\boldsymbol{\nu}}\right) + \boldsymbol{N}'\left(\frac{1}{U}\boldsymbol{T}^{-1}\boldsymbol{\nu}\right) + \boldsymbol{G}'\left(\frac{1}{L}\boldsymbol{T}^{-1}\boldsymbol{\eta}\right) = \frac{1}{\frac{1}{2}\rho U^2 L^2}\boldsymbol{T}\boldsymbol{\tau} \tag{7.80}$$

such that

$$(\boldsymbol{T}\boldsymbol{M}'\boldsymbol{T}^{-1})\dot{\boldsymbol{\nu}} + \left(\frac{U}{L}\right)(\boldsymbol{T}\boldsymbol{N}'\boldsymbol{T}^{-1})\boldsymbol{\nu} + \left(\frac{U}{L}\right)^2(\boldsymbol{T}\boldsymbol{G}'\boldsymbol{T}^{-1})\boldsymbol{\eta} = \frac{1}{\frac{1}{2}\rho L^3}\boldsymbol{T}^2\boldsymbol{\tau} \tag{7.81}$$

Hence,

$$\boldsymbol{M} = \frac{\rho L^3}{2}\boldsymbol{T}^{-2}(\boldsymbol{T}\boldsymbol{M}'\boldsymbol{T}^{-1}),$$

$$\boldsymbol{N} = \frac{\rho L^2 U}{2}\boldsymbol{T}^{-2}(\boldsymbol{T}\boldsymbol{N}'\boldsymbol{T}^{-1}),$$

$$\boldsymbol{G} = \frac{\rho L U^2}{2}\boldsymbol{T}^{-2}(\boldsymbol{T}\boldsymbol{G}'\boldsymbol{T}^{-1})$$

Table 7.3 6 DOF normalization variables

	Prime system	Bis system
Acceleration	$\dot{\boldsymbol{\nu}} = \frac{U^2}{L}\,\boldsymbol{T}\dot{\boldsymbol{\nu}}'$	$\dot{\boldsymbol{\nu}} = g\,\boldsymbol{T}\dot{\boldsymbol{\nu}}''$
Velocity	$\boldsymbol{\nu} = U\,\boldsymbol{T}\boldsymbol{\nu}'$	$\boldsymbol{\nu} = \sqrt{Lg}\,\boldsymbol{T}\boldsymbol{\nu}''$
Position/attitude	$\boldsymbol{\eta} = L\,\boldsymbol{T}\boldsymbol{\eta}'$	$\boldsymbol{\eta} = L\,\boldsymbol{T}\boldsymbol{\eta}''$
Control forces/moments	$\boldsymbol{\tau} = \frac{1}{2}\rho U^2 L^2\,\boldsymbol{T}^{-1}\boldsymbol{\tau}'$	$\boldsymbol{\tau} = \mu\rho g\nabla\,\boldsymbol{T}^{-1}\boldsymbol{\tau}''$

Notice that $\boldsymbol{\nu}$, $\boldsymbol{\eta}$ and the input vector $\boldsymbol{\tau}$ now have physical dimensions while $\boldsymbol{M}'$, $\boldsymbol{N}'$ and $\boldsymbol{G}'$ are nondimensional. Similarly, *bis system* scaling with $\mu = 1$ gives

$$(\boldsymbol{T}\boldsymbol{M}''\boldsymbol{T}^{-1})\dot{\boldsymbol{\nu}} + \sqrt{\frac{g}{L}}\,(\boldsymbol{T}\boldsymbol{N}''\boldsymbol{T}^{-1})\boldsymbol{\nu} + \frac{g}{L}\,(\boldsymbol{T}\boldsymbol{G}''\boldsymbol{T}^{-1})\boldsymbol{\eta} = \frac{1}{m}\boldsymbol{T}^2\boldsymbol{\tau} \tag{7.82}$$

Hence,

$$\begin{aligned}
\boldsymbol{M} &= m\boldsymbol{T}^{-2}(\boldsymbol{T}\boldsymbol{M}''\boldsymbol{T}^{-1}),\\
\boldsymbol{N} &= m\sqrt{\frac{g}{L}}\,\boldsymbol{T}^{-2}(\boldsymbol{T}\boldsymbol{N}''\boldsymbol{T}^{-1}),\\
\boldsymbol{G} &= m\frac{g}{L}\,\boldsymbol{T}^{-2}(\boldsymbol{T}\boldsymbol{G}''\boldsymbol{T}^{-1})
\end{aligned}$$

The 6 DOF normalization procedure is summarized in Table 7.3. The following example demonstrates this for a linearized maneuvering model.

Example 7.5 (Normalization of Parameters while keeping the Actual States)
Consider the model in Example 7.4:

$$\boldsymbol{M}'\dot{\boldsymbol{\nu}}' + \boldsymbol{N}'(u_0')\boldsymbol{\nu}' = \boldsymbol{b}'\delta' \tag{7.83}$$

Transforming the states $\boldsymbol{\nu}'$ and control input δ' in (7.80) to dimensional quantities yields

$$(\boldsymbol{T}\boldsymbol{M}'\boldsymbol{T}^{-1})\dot{\boldsymbol{\nu}} + \frac{U}{L}(\boldsymbol{T}\boldsymbol{N}'(u_0')\boldsymbol{T}^{-1})\boldsymbol{\nu} = \frac{U^2}{L}\boldsymbol{T}\boldsymbol{b}'\delta \tag{7.84}$$

where

$$\boldsymbol{T} = \mathrm{diag}\{1,\, 1/L\} \tag{7.85}$$

Notice that $\delta = \delta'$. Expanding (7.84) yields

$$\begin{bmatrix} m_{11}' & Lm_{12}' \\ \frac{1}{L}m_{21}' & m_{22}' \end{bmatrix}\begin{bmatrix} \dot{v} \\ \dot{r} \end{bmatrix} + \frac{U}{L}\begin{bmatrix} n_{11}' & Ln_{12}' \\ \frac{1}{L}n_{21}' & n_{22}' \end{bmatrix}\begin{bmatrix} v \\ r \end{bmatrix} = \frac{U^2}{L}\begin{bmatrix} b_1' \\ \frac{1}{L}\,b_2' \end{bmatrix}\delta \tag{7.86}$$

where m_{ij}', d_{ij}' and b_i' are defined according to prime systems I or II in Table 7.2.

Example 7.6 (Normalization Procedure for the Nomoto Time and Gain Constants)
The gain and time constants in Nomoto's first- and second-order models can be made invariant with respect to L and U by using

$$K' = (L/U)\,K, \quad T' = (U/L)\,T \tag{7.87}$$

This suggests that the first-order ship dynamics can be expressed as

$$(L/U)\,T'\,\dot{r} + r = (U/L)\,K'\,\delta \tag{7.88}$$

or

$$\dot{r} = -\left(\frac{U}{L}\right)\frac{1}{T'}r + \left(\frac{U}{L}\right)^2\frac{K'}{T'}\delta \tag{7.89}$$

This representation is quite useful since the nondimensional gain and time constants will typically be in the range $0.5 < K' < 2$ *and* $0.5 < T' < 2$ *for most ships. An extension to Nomoto's second-order model is obtained by writing*

$$(L/U)^2\,T_1'\,T_2'\,\psi^{(3)} + (L/U)\,(T_1' + T_2')\,\ddot{\psi} + \dot{\psi} = (U/L)\,K'\,\delta + K'\,T_3'\,\dot{\delta} \tag{7.90}$$

where the nondimensional time constants T_i' *are defined as* $T_i' = T_i\,(U/L)$ *for* $(i = 1, 2, 3)$ *and the nondimensional gain constant is* $K' = (L/U)\,K$.

7.3 DP Models (3 DOF)

Models for dynamic positioning (DP) are derived under the assumption of low speed. The DP models are valid for stationkeeping and low-speed maneuvering up to approximately 2 m/s, as indicated by the speed regions shown in Figure 7.2. This section presents a nonlinear DP model based on current coefficients and linear exponential damping that can be used for accurate simulation and prediction. In addition to this, a linearized model intended for controller–observer design is derived.

Consider the nonlinear model:

$$\dot{\boldsymbol{\eta}} = \boldsymbol{R}(\psi)\boldsymbol{\nu} \tag{7.91}$$

$$\boldsymbol{M}\dot{\boldsymbol{\nu}} + \boldsymbol{C}_{RB}(\boldsymbol{\nu})\boldsymbol{\nu} + \boldsymbol{N}(\boldsymbol{\nu}_r)\boldsymbol{\nu}_r = \boldsymbol{\tau} + \boldsymbol{\tau}_{\text{wind}} + \boldsymbol{\tau}_{\text{wave}} \tag{7.92}$$

where

$$\boldsymbol{N}(\boldsymbol{\nu}_r)\boldsymbol{\nu}_r := \boldsymbol{C}_A(\boldsymbol{\nu}_r)\boldsymbol{\nu}_r + \boldsymbol{D}(\boldsymbol{\nu}_r)\boldsymbol{\nu}_r \tag{7.93}$$

The state vectors are $\boldsymbol{\nu} = [u, v, r]^\top$ and $\boldsymbol{\eta} = [N, E, \psi]^\top$. This implies that the dynamics associated with the motion in heave, roll and pitch are neglected, that is $w = p = q = 0$.

The rotation, mass and Coriolis–centripetal matrices for DP are

$$\boldsymbol{R}(\psi) = \begin{bmatrix} \cos(\psi) & -\sin(\psi) & 0 \\ \sin(\psi) & \cos(\psi) & 0 \\ 0 & 0 & 1 \end{bmatrix} \tag{7.94}$$

$$\boldsymbol{M} = \begin{bmatrix} m - X_{\dot{u}} & 0 & 0 \\ 0 & m - Y_{\dot{v}} & mx_g - Y_{\dot{r}} \\ 0 & mx_g - Y_{\dot{r}} & I_z - N_{\dot{r}} \end{bmatrix} \tag{7.95}$$

$$\boldsymbol{C}_{RB}(\boldsymbol{\nu}) = \begin{bmatrix} 0 & 0 & -m(x_g r + v) \\ 0 & 0 & mu \\ m(x_g r + v) & -mu & 0 \end{bmatrix} \tag{7.96}$$

Notice that surge is decoupled from sway and yaw is due to symmetry considerations of the system inertia matrix (Section 3.3). It is assumed that the added mass matrix is computed in CO. The expression for $\boldsymbol{N}(\boldsymbol{\nu}_r)$ will depend on how the dissipative forces are modeled. This is the topic for the next sections.

7.3.1 Nonlinear DP Model using Current Coefficients

For low-speed applications such as DP, ocean currents and damping can be modeled by three *current coefficients* C_X, C_Y and C_N. These can be experimentally obtained using scale models in wind tunnels. The resulting forces are measured on the model, which is restrained from moving ($U = 0$). The current coefficients can also be related to the surge resistance, cross-flow drag and the Munk moment used in maneuvering theory. For a ship moving at forward speed $U > 0$, quadratic damping will be embedded in the current coefficients if relative speed is used.

Zero-Speed Representation

In many textbooks and papers, for instance Blendermann (1994), wind and current coefficients are defined in $\{b\}$ relative to the bow using a *counter clockwise rotation* γ_c (see Figure 7.5). The current forces on a

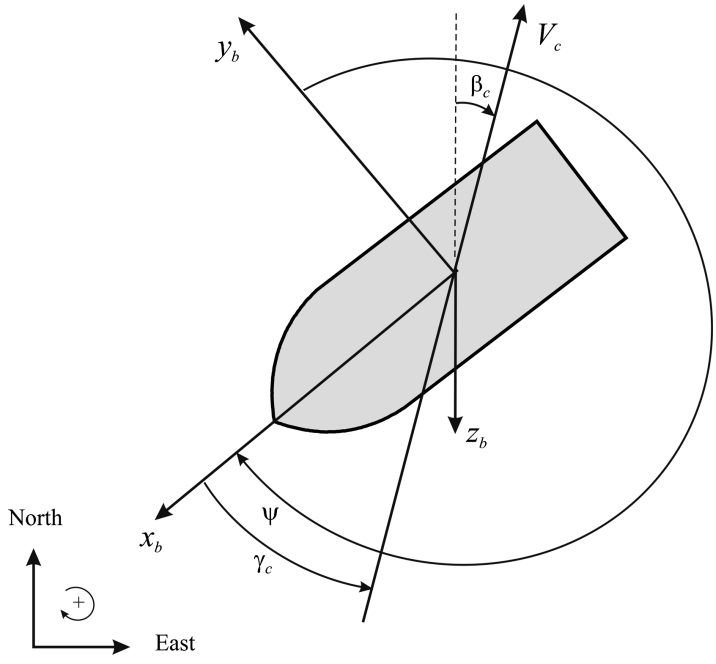

Figure 7.5 Current speed V_c, current direction β_c and current angle of attack γ_c relative to the bow.

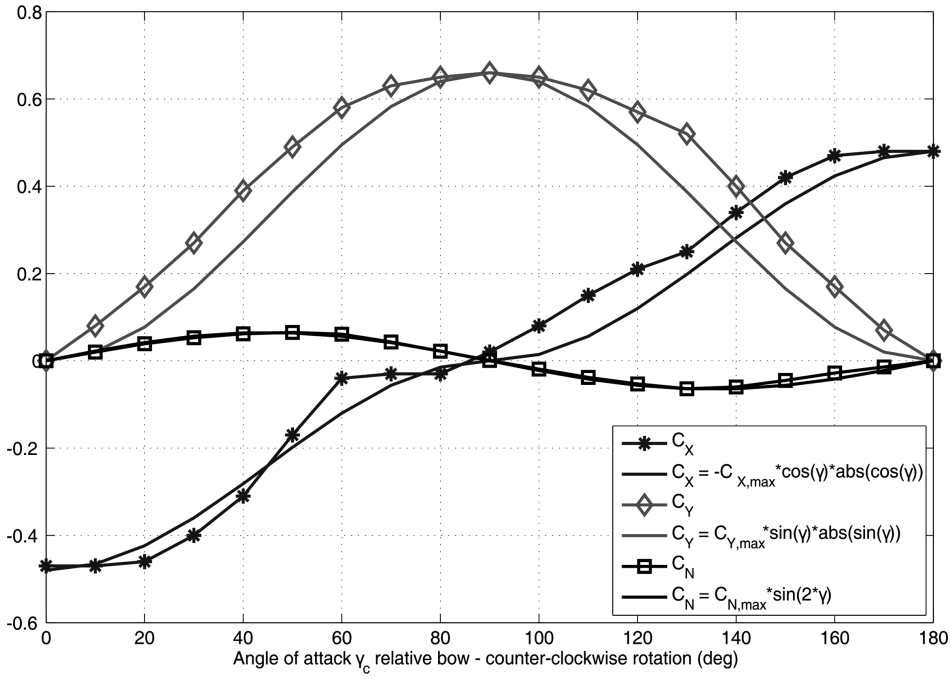

Figure 7.6 Experimental current coefficients C_X, C_Y and C_N for a tanker. Notice that γ_c is a counter clockwise rotation and the angle of attack $\gamma_c = 0^\circ$ for a current in the bow.

marine craft at rest ($U = 0$) can be expressed in terms of the area-based current coefficients $C_X(\gamma_c)$, $C_Y(\gamma_c)$ and $C_N(\gamma_c)$ as

$$X_{\text{current}} = \frac{1}{2}\rho A_{Fc} C_X(\gamma_c) V_c^2 \tag{7.97}$$

$$Y_{\text{current}} = \frac{1}{2}\rho A_{Lc} C_Y(\gamma_c) V_c^2 \tag{7.98}$$

$$N_{\text{current}} = \frac{1}{2}\rho A_{Lc} L_{oa} C_N(\gamma_c) V_c^2 \tag{7.99}$$

where V_c is the speed of the ocean current. The frontal and lateral projected currents areas are denoted A_{Fc} and A_{Lc}, respectively, while L_{oa} is the length overall and ρ is the density of water. Typical experimental current coefficients are shown in Figure 7.6.

Forward Speed Representation

Equations (7.97)–(7.99) only add zero-speed current forces (no damping) to the equations of motion since they only depend on the current speed V_c. For a ship moving at relative forward speed, $U_r > 0$, current forces and quadratic damping in surge and sway are given by

$$X_{\text{current}} = \frac{1}{2}\rho A_{Fc} C_X(\gamma_{rc}) V_{rc}^2 \tag{7.100}$$

$$Y_{\text{current}} = \frac{1}{2}\rho A_{Lc} C_Y(\gamma_{rc}) V_{rc}^2 \tag{7.101}$$

$$N_{\text{current}} = \frac{1}{2}\rho A_{Lc} L_{oa} C_N(\gamma_{rc}) V_{rc}^2 \tag{7.102}$$

These expressions are functions of the relative speed V_{rc} and direction γ_{rc}:

$$V_{rc} = \sqrt{u_{rc}^2 + v_{rc}^2} = \sqrt{(u - u_c)^2 + (v - v_c)^2} \tag{7.103}$$

$$\gamma_{rc} = -\text{atan2}(v_{rc}, u_{rc}) \tag{7.104}$$

where

$$u_c = V_c \cos(\beta_c - \psi) \tag{7.105}$$

$$v_c = V_c \sin(\beta_c - \psi) \tag{7.106}$$

are the current velocities (see Section 8.3).

Ocean Current Angle of Attack

From Figure 7.5, it is seen that the angles assosiated with an ocean current in the horizontal plane for a marine craft at rest satisfy

$$\gamma_c = \psi - \beta_c - \pi \tag{7.107}$$

where β_c is the direction of the ocean current and γ_c is specified relative to the bow. Hence, the velocity components (7.105) and (7.106) can be written

$$u_c = -V_c \cos(\gamma_c) \tag{7.108}$$

$$v_c = V_c \sin(\gamma_c) \tag{7.109}$$

The current goes in the geographic direction β_c in $\{n\}$ and its magnitude is

$$V_c = \sqrt{u_c^2 + v_c^2} \tag{7.110}$$

Notice that for zero speed the expressions (7.103) and (7.104) become

$$V_{rc} = \sqrt{(u - u_c)^2 + (v - v_c)^2} \overset{u=v=0}{=} V_c \tag{7.111}$$

$$\tan(\gamma_{rc}) = -\frac{v - v_c}{u - v_c} \overset{u=v=0}{=} -\frac{v_c}{u_c} = \tan(\gamma_c) \tag{7.112}$$

This means that the angles γ_{rc} and γ_c as well as the speeds V_{rc} and V_c in general are different for $U > 0$. Consequently, the geometrical relationship (7.107) shown in Figure 7.5 only holds for $U = 0$.

Relationship Between Current Coefficients and Surge Resistance/Cross-Flow Drag

The current coefficients can be related to the surge resistance (6.86) and cross-flow drag (6.94)–(6.95) coefficients by assuming low speed such that $u \approx 0$ and $v \approx 0$. This is a good assumption for DP. From (7.108)–(7.109) it follows that the quadratic terms are

$$\begin{aligned} u_r\,|u_r| &\approx -u_c\,|-u_c| \\ &= V_c^2 \cos(\gamma_c)|\cos(\gamma_c)| \end{aligned} \tag{7.113}$$

$$\begin{aligned} v_r\,|v_r| &\approx -v_c\,|-v_c| \\ &= -V_c^2 \sin(\gamma_c)|\sin(\gamma_c)| \end{aligned} \tag{7.114}$$

$$\begin{aligned} u_r v_r &\approx u_c v_c \\ &= -\frac{1}{2} V_c^2 \sin(2\gamma_c) \end{aligned} \tag{7.115}$$

The next step is to neglect terms in r (no rotations during stationkeeping) in (6.94)–(6.95) and require that C_X, C_Y and C_N in (7.97)–(7.99) satisfy

$$X_{\text{current}} = \frac{1}{2}\rho A_{Fc} C_X(\gamma_c) V_c^2 := X_{|u|u}\,|u_r|\,u_r \tag{7.116}$$

$$Y_{\text{current}} = \frac{1}{2}\rho A_{Lc} C_Y(\gamma_c) V_c^2 := Y_{|v|v}|v_r|v_r \tag{7.117}$$

$$N_{\text{current}} = \frac{1}{2}\rho A_{Lc} L_{oa} C_N(\gamma_c) V_c^2 := N_{|v|v}|v_r|v_r - \underbrace{(X_{\dot{u}} - Y_{\dot{v}})u_r v_r}_{\text{Munk moment}} \tag{7.118}$$

for $u = v = r = 0$. Notice that the Munk moment $(Y_{\dot{v}} - X_{\dot{u}})u_r v_r$ in the yaw equation is included in the expression for N_{current} (see Section 7.1.4). The other terms are recognized as diagonal quadratic damping terms in $\boldsymbol{D}(\boldsymbol{\nu}_r)$.

This gives the following analytical expressions for the area-based current coefficients:

$$C_X(\gamma_c) = -2\left(\frac{-X_{|u|u}}{\rho A_{Fc}}\right)\cos(\gamma_c)|\cos(\gamma_c)| \tag{7.119}$$

$$C_Y(\gamma_c) = 2\left(\frac{-Y_{|v|v|}}{\rho A_{Lc}}\right)\sin(\gamma_c)|\sin(\gamma_c)| \tag{7.120}$$

$$C_N(\gamma_c) = \frac{2}{\rho A_{Lc} L_{oa}}(-N_{|v|v}\sin(\gamma_c)|\sin(\gamma_c)| + \frac{1}{2}\underbrace{(X_{\dot{u}} - Y_{\dot{v}})}_{A_{22}-A_{11}}\sin(2\gamma_c)) \tag{7.121}$$

These results are similar to Faltinsen (1990, pp. 187–188). The trigonometric functions in (7.119)–(7.121) will be quite close to the shape of the experimental current coefficients shown in Figure 7.6. For tankers, the current coefficients can be computed using the formulae of Leite *et al.* (1998) whereas the ITTC and cross-flow drag principles are commonly used for other hull forms.

The nonlinear DP model based on current coefficients takes the following form:

$$\dot{\boldsymbol{\eta}} = \boldsymbol{R}(\psi)\boldsymbol{\nu} \tag{7.122}$$

$$\boldsymbol{M}\dot{\boldsymbol{\nu}} + \boldsymbol{C}_{RB}(\boldsymbol{\nu})\boldsymbol{\nu} + \boldsymbol{D}\exp(-\alpha V_{rc})\boldsymbol{\nu}_r + \boldsymbol{d}(V_{rc}, \gamma_{rc}) = \boldsymbol{\tau} + \boldsymbol{\tau}_{\text{wind}} + \boldsymbol{\tau}_{\text{wave}} \tag{7.123}$$

$$\boldsymbol{d}(V_{rc}, \gamma_{cr}) = \begin{bmatrix} -\frac{1}{2}\rho A_{Fc} C_X(\gamma_{rc}) V_{rc}^2 \\ -\frac{1}{2}\rho A_{Lc} C_Y(\gamma_{rc}) V_{rc}^2 \\ -\frac{1}{2}\rho A_{Lc} L_{oa} C_N(\gamma_{rc}) V_{rc}^2 - N_{|r|r} r|r \end{bmatrix} \tag{7.124}$$

where $-N_{|r|r} > 0$ is an optional quadratic damping coefficient used to counteract the destabilizing Munk moment in yaw since the current coefficients do not include nonlinear damping in yaw. The model also includes an optional linear damping matrix:

$$\boldsymbol{D} = \begin{bmatrix} -X_u & 0 & 0 \\ 0 & -Y_v & -Y_r \\ 0 & -N_v & -N_r \end{bmatrix} \tag{7.125}$$

to ensure exponential convergence at low relative speed V_r. This is done by tuning $\alpha > 0$. At higher speeds $V_{rc} \gg 0$ and the nonlinear term $\boldsymbol{d}(V_{rc}, \gamma_{rc})$ dominates over the linear term, which vanishes at higher speeds.

It is also possible to eliminate $\boldsymbol{\nu}$ in (7.123) by using Property 8.1 in Section 8.3. The key assumption is that $\boldsymbol{C}_{RB}(\boldsymbol{\nu})$ must be parametrized according to (3.57). Hence, it follows that

$$\boldsymbol{M}\dot{\boldsymbol{\nu}}_r + \boldsymbol{C}_{RB}(\boldsymbol{\nu}_r)\boldsymbol{\nu}_r + \boldsymbol{D}\exp(-\alpha V_{rc})\boldsymbol{\nu}_r + \boldsymbol{d}(V_{rc}, \gamma_{rc}) = \boldsymbol{\tau} + \boldsymbol{\tau}_{\text{wind}} + \boldsymbol{\tau}_{\text{wave}} \tag{7.126}$$

where $\boldsymbol{\nu}_r$ is the state vector.

7.3.2 Linearized DP Model

As shown in Section 6.4, linear damping is a good assumption for low-speed applications. Similarly, the quadratic velocity terms given by $\boldsymbol{C}(\boldsymbol{\nu}_r)\boldsymbol{\nu}_r$ and $\boldsymbol{d}(V_{rc}, \gamma_{rc})$ can be neglected when designing DP control systems if the ocean currents (drift) are properly compensated for by using integral action. One way to do this is to treat the ocean currents as a slowly varying bias vector $\boldsymbol{b}$ expressed in $\{n\}$. Hence, the relative velocity vector $\boldsymbol{\nu}_r$ is superfluous. The linear model is usually expressed in *vessel parallel coordinates* (see Section 7.5.3):

$$\boldsymbol{\eta}_p = \boldsymbol{R}^\top(\psi)\boldsymbol{\eta} \tag{7.127}$$

such that

$$\dot{\boldsymbol{\eta}}_p = \boldsymbol{\nu} \tag{7.128}$$

$$\boldsymbol{M}\dot{\boldsymbol{\nu}} + \boldsymbol{D}\boldsymbol{\nu} = \boldsymbol{R}^\top(\psi)\boldsymbol{b} + \boldsymbol{\tau} + \boldsymbol{\tau}_{\text{wind}} + \boldsymbol{\tau}_{\text{wave}} \tag{7.129}$$

$$\dot{\boldsymbol{b}} = \boldsymbol{0} \tag{7.130}$$

where

$$\boldsymbol{\tau} = \boldsymbol{B}\boldsymbol{u} \tag{7.131}$$

This model is intended for controller–observer design, where feedback suppresses errors due to the model uncertainty. The control matrix $\boldsymbol{B}$ describes the thruster configuration while $\boldsymbol{u}$ is the control input vector. Notice that the currents are assumed constant in $\{n\}$ and therefore transformed to $\{b\}$ by $\boldsymbol{R}^\top(\psi)\boldsymbol{b}$. The position reference signals $\boldsymbol{y} = \boldsymbol{\eta}$ are transformed to vessel parallel coordinates $\boldsymbol{\eta}_p$ at each time step using (7.127). This removes the kinematic nonlinearity.

7.4 Maneuvering Models including Roll (4 DOF)

The maneuvering models presented in Section 7.1 only describe the horizontal motions (*surge, sway* and *yaw*). These models are intended for the design and simulation of DP systems, heading autopilots, trajectory-tracking and path-following control systems. Many vessels, however, are equipped with actuators that can reduce the rolling motion. This could be anti-rolling tanks, rudders and fin stabilizers (see Part II). In order to design a control system for roll damping, it is necessary to add the roll equation to the horizontal plane model. Inclusion of roll means that the restoring moment due to buoyancy and gravity must be included. The resulting model is a 4 DOF maneuvering model that includes roll (*surge, sway, roll* and *yaw*).

The speed equation (7.32) can be decoupled from the sway, roll and yaw modes. The resulting model takes the form

$$\boldsymbol{M}\dot{\boldsymbol{\nu}} + \boldsymbol{N}(u_o)\boldsymbol{\nu} + \boldsymbol{G}\boldsymbol{\eta} = \boldsymbol{\tau} \tag{7.132}$$

where $u_o = \text{constant}$, $\boldsymbol{\nu} = [v, p, r]^\top$ and $\boldsymbol{\eta} = [E, \phi, \psi]^\top$ are the states while $\boldsymbol{\tau}$ is the control vector. For a ship with homogeneous mass distribution and xz-plane symmetry, $I_{xy} = I_{yz} = 0$ and $y_g = 0$.

From the general expressions (3.44) and (6.38) in Sections 3.3 and 6.3.1, respectively, we get (with nonzero I_{xz})

$$\boldsymbol{M} = \begin{bmatrix} m - Y_{\dot{v}} & -mz_g - Y_{\dot{p}} & mx_g - Y_{\dot{r}} \\ -mz_g - K_{\dot{v}} & I_x - K_{\dot{p}} & -I_{xz} - K_{\dot{r}} \\ mx_g - N_{\dot{v}} & -I_{xz} - N_{\dot{p}} & I_z - N_{\dot{r}} \end{bmatrix} \tag{7.133}$$

The expression for $\boldsymbol{N}(u_o)$ is obtained by linearization of $\boldsymbol{C}(\boldsymbol{\nu})$ and $\boldsymbol{D}(\boldsymbol{\nu})$ about $u = u_0$ which gives

$$\boldsymbol{N}(u_o) = \begin{bmatrix} -Y_v & -Y_p & mu_0 - Y_r \\ -K_v & -K_p & -mz_g u_0 - K_r \\ -N_v & -N_p & mx_g u_0 - N_r \end{bmatrix} \tag{7.134}$$

Recall from Section 4.1 that the linear restoring forces and moments for a surface vessel can be written

$$\boldsymbol{G} = \text{diag}\{0, W\overline{GM}_T, 0\} \tag{7.135}$$

where $W = mg$ is the weight and $\overline{GM}_T$ is the transverse metacenter height.

In addition to these equations, the kinematic equations (assuming $q = \theta = 0$)

$$\dot{\phi} = p \tag{7.136}$$

$$\dot{\psi} = \cos(\phi) r \approx r \tag{7.137}$$

must be augmented to the system model. The general kinematic expressions are found in Section 2.2.1.

State-Space Model

The linearized model (7.132) together with (7.136)–(7.137) can be written in state-space form by defining the state vector as $\boldsymbol{x} := [v,\, p,\, r,\, \phi,\, \psi]^\top$. The elements associated with the matrices $\boldsymbol{A}$ and $\boldsymbol{B}$ are given by

$$\dot{\boldsymbol{x}} = \underbrace{\begin{bmatrix} a_{11} & a_{12} & a_{13} & a_{14} & 0 \\ a_{21} & a_{22} & a_{23} & a_{24} & 0 \\ a_{31} & a_{32} & a_{33} & a_{34} & 0 \\ 0 & 1 & 0 & 0 & 0 \\ 0 & 0 & 1 & 0 & 0 \end{bmatrix}}_{\boldsymbol{A}} \boldsymbol{x} + \underbrace{\begin{bmatrix} b_{11} & b_{12} & \cdots & b_{1r} \\ b_{21} & b_{22} & \cdots & b_{2r} \\ b_{31} & b_{32} & \cdots & b_{3r} \\ 0 & 0 & \cdots & 0 \\ 0 & 0 & \cdots & 0 \end{bmatrix}}_{\boldsymbol{B}} \boldsymbol{u} \tag{7.138}$$

where the elements a_{ij} are found from

$$\begin{bmatrix} a_{11} & a_{12} & a_{13} \\ a_{21} & a_{22} & a_{23} \\ a_{31} & a_{32} & a_{33} \end{bmatrix} = -\boldsymbol{M}^{-1}\boldsymbol{N}(u_o) \tag{7.139}$$

$$\begin{bmatrix} * & a_{14} & * \\ * & a_{24} & * \\ * & a_{34} & * \end{bmatrix} = -\boldsymbol{M}^{-1}\boldsymbol{G} \tag{7.140}$$

while the elements b_{ij} depend on what type of actuators are in use. Finally, the roll and yaw outputs are chosen as

$$\phi = \underbrace{[0, 0, 0, 1, 0]}_{\boldsymbol{c}_{\text{roll}}^\top} \boldsymbol{x} \tag{7.141}$$

$$\psi = \underbrace{[0, 0, 0, 0, 1]}_{\boldsymbol{c}_{\text{yaw}}^\top} \boldsymbol{x} \tag{7.142}$$

Decompositions in Roll and Sway–Yaw Subsystems

To simplify the system for further analysis, the state vector is reorganized such that state variables associated with the steering and roll dynamics are separated. Consequently, (7.138) is rewritten as

$$\begin{bmatrix} \dot{v} \\ \dot{r} \\ \dot{\psi} \\ \hline \dot{p} \\ \dot{\phi} \end{bmatrix} = \left[\begin{array}{ccc|cc} a_{11} & a_{13} & 0 & a_{12} & a_{14} \\ a_{31} & a_{33} & 0 & a_{32} & a_{34} \\ 0 & 1 & 0 & 0 & 0 \\ \hline a_{21} & a_{23} & 0 & a_{22} & a_{24} \\ 0 & 0 & 0 & 1 & 0 \end{array}\right] \begin{bmatrix} v \\ r \\ \psi \\ \hline p \\ \phi \end{bmatrix} + \begin{bmatrix} b_{11} & b_{12} & \cdots & b_{1r} \\ b_{31} & b_{32} & \cdots & b_{3r} \\ 0 & 0 & \cdots & 0 \\ b_{21} & b_{22} & \cdots & b_{2r} \\ 0 & 0 & \cdots & 0 \end{bmatrix} \boldsymbol{u} \tag{7.143}$$

Let

$$\begin{bmatrix} \dot{\boldsymbol{x}}_\psi \\ \dot{\boldsymbol{x}}_\phi \end{bmatrix} = \begin{bmatrix} \boldsymbol{A}_{\psi\psi} & \boldsymbol{A}_{\psi\phi} \\ \boldsymbol{A}_{\phi\psi} & \boldsymbol{A}_{\phi\phi} \end{bmatrix} \begin{bmatrix} \boldsymbol{x}_\psi \\ \boldsymbol{x}_\phi \end{bmatrix} + \begin{bmatrix} \boldsymbol{B}_\psi \\ \boldsymbol{B}_\phi \end{bmatrix} \boldsymbol{u} \tag{7.144}$$

where $\boldsymbol{x}_\psi = [v, r, \psi]^\top$ and $\boldsymbol{x}_\phi = [p, \phi]^\top$.

If the coupling matrices are small, that is $\boldsymbol{A}_{\psi\phi} = \boldsymbol{A}_{\phi\psi} = \boldsymbol{0}$, the following subsystems:

$$\begin{bmatrix} \dot{p} \\ \dot{\phi} \end{bmatrix} = \begin{bmatrix} a_{22} & a_{24} \\ 1 & 0 \end{bmatrix} \begin{bmatrix} p \\ \phi \end{bmatrix} + \begin{bmatrix} b_{21} & b_{22} & \cdots & b_{2r} \\ 0 & 0 & \cdots & 0 \end{bmatrix} \boldsymbol{u} \tag{7.145}$$

and

$$\begin{bmatrix} \dot{v} \\ \dot{r} \\ \dot{\psi} \end{bmatrix} = \begin{bmatrix} a_{11} & a_{13} & 0 \\ a_{31} & a_{33} & 0 \\ 0 & 1 & 0 \end{bmatrix} \begin{bmatrix} v \\ r \\ \psi \end{bmatrix} + \begin{bmatrix} b_{11} & b_{12} & \cdots & b_{1r} \\ b_{31} & b_{32} & \cdots & b_{3r} \\ 0 & 0 & \cdots & 0 \end{bmatrix} \boldsymbol{u} \tag{7.146}$$

will describe the ship dynamics. The last expression is recognized as the second-order Nomoto model (7.46) with r control inputs.

Transfer Functions for Steering and Rudder-Roll Damping

The linearized model (7.143) is useful for frequency analysis of rudder-roll damping (RRD) systems. For simplicity consider a ship with one rudder $u = \delta$ and $\boldsymbol{b} = [b_{11}, b_{21}, b_{31}, 0, 0]^\top$. For the state-space model (7.143) the transfer functions $\phi(s)/\delta(s) = \boldsymbol{c}_{\text{roll}}^\top (s\boldsymbol{I} - \boldsymbol{A})^{-1}\boldsymbol{b}$ and $\psi(s)/\delta(s) = \boldsymbol{c}_{\text{yaw}}^\top (s\boldsymbol{I} - \boldsymbol{A})^{-1}\boldsymbol{b}$ become

$$\frac{\phi}{\delta}(s) = \frac{b_2 s^2 + b_1 s + b_0}{s^4 + a_3 s^3 + a_2 s^2 + a_1 s + a_0} \approx \underbrace{\frac{K_{\text{roll}}\, \omega_{\text{roll}}^2\, (1 + T_5 s)}{(1 + T_4 s)(s^2 + 2\zeta\omega_{\text{roll}} s + \omega_{\text{roll}}^2)}}_{\text{no coupling between roll and sway–yaw}} \tag{7.147}$$

$$\frac{\psi}{\delta}(s) = \frac{c_3 s^3 + c_2 s^2 + c_1 s + c_0}{s(s^4 + a_3 s^3 + a_2 s^2 + a_1 s + a_0)} \approx \underbrace{\frac{K_{\text{yaw}}\, (1 + T_3 s)}{s(1 + T_1 s)(1 + T_2 s)}}_{\text{no coupling between roll and sway–yaw}} \tag{7.148}$$

where the decoupled models (7.145) and (7.146) have been applied. In most cases, this approximation is only rough so care should be taken. In Figure 7.7 it is seen that the phase of the roll transfer function

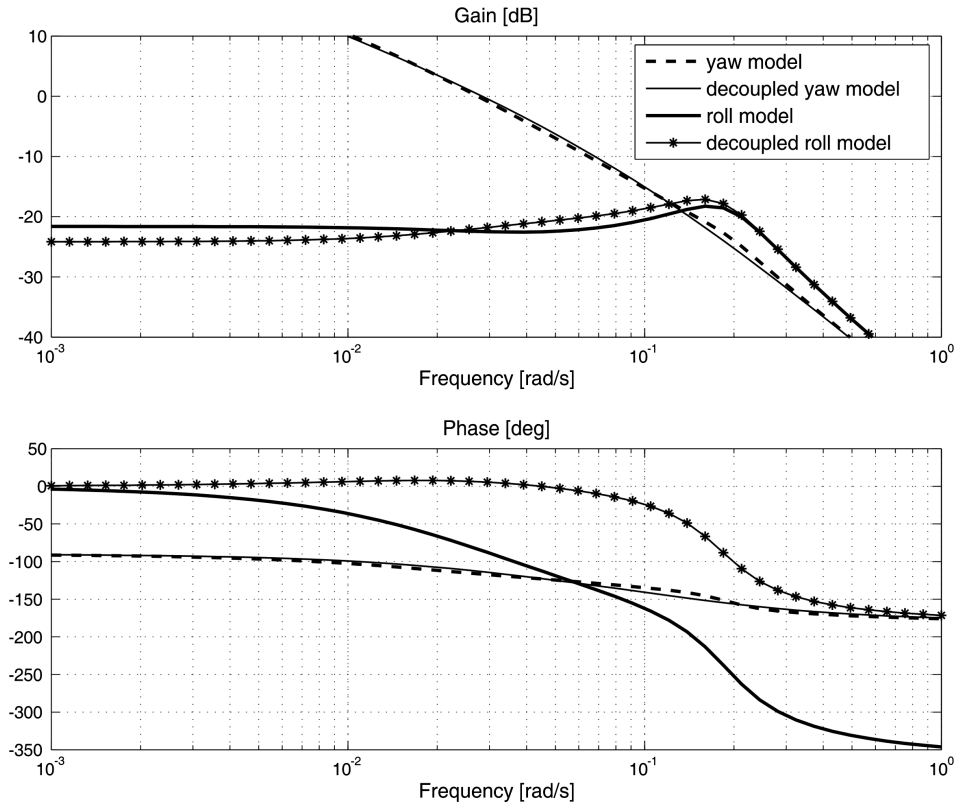

Figure 7.7 Transfer functions for the roll and sway–yaw subsystems corresponding to the Son and Nomoto container ship.

is inaccurate for the decoupled model. This can be improved by using a model reduction via a balanced state-space realization (see modred.m and ssbal.m in Matlab).

Also, parametric investigations show that cross-couplings between steering and roll might give robust performance problems of RRD control systems (Blanke and Christensen, 1993). This is also documented in Blanke (1996), who has identified the ship parameters for several loading conditions during sea trials with a series of ships. The results clearly reveal changes in the dynamics between the different ships in the series, indicating that there is a robustness problem due to changes in load conditions and rudder shape. Nonlinear effects also give rise to the same problem. Identification of ship steering-roll models are discussed by Blanke and Tiano (1997). The interested reader is also advised to consult Van der Klugt (1987) for a discussion of decoupled linear models for RRD, while nonlinear models are presented in Section 7.4.1.

Example 7.7 (Roll and Sway–Yaw Transfer Functions)
The roll and yaw transfer functions corresponding to the model of Son and Nomoto (1981) are plotted in Figure 7.7 using the MSS toolbox file ExRRD1.m. The plots show both the full state-space model (7.138) and the decoupled models (7.145)–(7.146). The model considered is a container ship of length $L = 175$ m *and with a displacement volume of* $21\ 222$ m^3. *The ship is moving at service speed*

$u_0 = 7.0$ m/s. *The model of Son and Nomoto (1981) is based on a third-order Taylor-series expansion (see Section 7.1.3) of the hydrodynamic forces including higher-order restoring terms replacing (7.135). The nonlinear model is included in the MSS toolbox under the file name container.m while a linearized version of this model is found in Lcontainer.m. The nonlinear model is described more closely in the next section. The numerical values for the transfer functions are*

$$\frac{\phi}{\delta}(s) = \frac{0.0032(s - 0.036)(s + 0.077)}{(s + 0.026)(s + 0.116)(s^2 + 0.136s + 0.036)} \approx \frac{0.083(1 + 49.1s)}{(1 + 31.5s)(s^2 + 0.134s + 0.033)} \tag{7.149}$$

and

$$\frac{\psi}{\delta}(s) = \frac{0.0024(s + 0.0436)(s^2 + 0.162s + 0.035)}{s(s + 0.0261)(s + 0.116)(s^2 + 0.136s + 0.036)} \approx \frac{0.032(1 + 16.9s)}{s(1 + 24.0s)(1 + 9.2s)} \tag{7.150}$$

corresponding to

$$\omega_{\text{roll}} = 0.189 \text{ rad/s} \tag{7.151}$$

$$\zeta = 0.36 \tag{7.152}$$

It is seen that the amplitudes of the roll and yaw models are quite close. However, the decoupled model in roll does not describe the phase with sufficient accuracy, so stability problems could be an issue when designing a model-based RRD. The main reason for this is that one pole–zero pair is omitted in the decoupled roll model. Since this is a right-half-plane zero,

$$z = 0.036 \text{ rad/s} \tag{7.153}$$

the pole–zero pair gives an additional phase lag of -180 *degrees, as observed in the plot of the full model. This will of course result in serious stability problems when trying to damp the roll motion.*

In practice it will be difficult to design an RRD for this system since the controller should reduce the energy at the peak frequency $\omega_{\text{roll}} = 0.189$ rad/s *which is much higher than the right-half-plane zero* $z = 0.036$ rad/s. *This is a nonminimum phase property which cannot be changed with feedback (recall that only poles and not zeros can be moved using feedback control). The nonminimum phase characteristic is observed as an inverse response in roll when a step input is applied (see Figure 7.8).*

The plots in Figure 7.8 are generated by simulating the nonlinear model of Son and Nomoto (see ExRRD3.m). The nonminimum phase behavior due to the right-half-plane zero is discussed in more detail by Fossen and Lauvdal (1994), where both linear and nonlinear analyses of the models of Son and Nomoto are considered. The nonlinear equivalent to a right-half-plane zero is unstable zero dynamics.

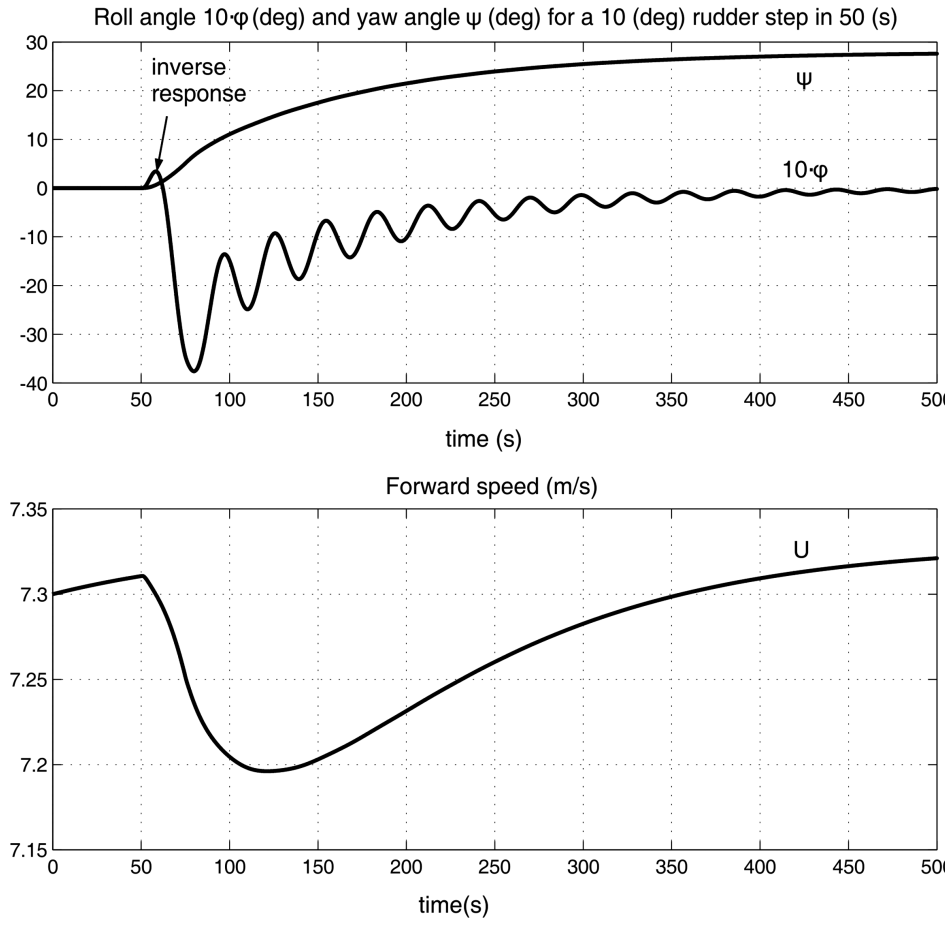

Figure 7.8 Roll angle $10\dot{\phi}$ and yaw angle ψ versus time for a 10 degree rudder step in 50 s. Notice the inverse response in roll and speed reduction during turning.

7.4.1 The Nonlinear Model of Son and Nomoto

A nonlinear model including roll for a high-speed container ship has been proposed by Son and Nomoto (1981, 1982):

$$(m + m_x)\dot{u} - (m + m_y)vr = X + \tau_1 \tag{7.154}$$

$$(m + m_y)\dot{v} + (m + m_x)ur + m_y\alpha_y\dot{r} - m_y l_y \dot{p} = Y + \tau_2 \tag{7.155}$$

$$(I_x + J_x)\dot{p} - m_y l_y \dot{v} - m_x l_x ur = K - W\overline{GM}_T\phi + \tau_4 \tag{7.156}$$

$$(I_z + J_z)\dot{r} + m_y\alpha_y\dot{v} = N - x_g Y + \tau_6 \tag{7.157}$$

where $m_x = A_{11}(0)$, $m_y = A_{22}(0)$, $J_x = A_{44}(\omega_{\text{roll}})$ and $J_z = A_{66}(0)$ denote the added mass and added moments of inertia. The control inputs are recognized as $\boldsymbol{\tau} = [\tau_1, \tau_2, \tau_4, \tau_6]^\top$. The added mass x

coordinates of m_x and m_y are denoted by α_x and α_y, while l_x and l_y are the added mass z coordinates of m_x and m_y, respectively.

The terms on the right-hand side of (7.154)–(7.157) are defined in terms of a third-order Taylor series expansion where small coefficients are neglected. The remaining terms are

$$X = X(u) + (1-t)T + X_{vr}vr + X_{vv}v^2 + X_{rr}r^2 + X_{\phi\phi}\phi^2 + X_\delta \sin\delta + X_{\text{ext}} \tag{7.158}$$

$$\begin{aligned} Y = {} & Y_v v + Y_r r + Y_\phi \phi + Y_p p + Y_{vvv}v^3 + Y_{rrr}r^3 + Y_{vvr}v^2 r + Y_{vrr}vr^2 \\ & + Y_{vv\phi}v^2\phi + Y_{v\phi\phi}v\phi^2 + Y_{rr\phi}r^2\phi + Y_{r\phi\phi}r\phi^2 + Y_\delta \cos\delta + Y_{\text{ext}} \end{aligned} \tag{7.159}$$

$$\begin{aligned} K = {} & K_v v + K_r r + K_\phi \phi + K_p p + K_{vvv}v^3 + K_{rrr}r^3 + K_{vvr}v^2 r + K_{vrr}vr^2 \\ & + K_{vv\phi}v^2\phi + K_{v\phi\phi}v\phi^2 + K_{rr\phi}r^2\phi + K_{r\phi\phi}r\phi^2 + K_\delta \cos\delta + K_{\text{ext}} \end{aligned} \tag{7.160}$$

$$\begin{aligned} N = {} & N_v v + N_r r + N_\phi \phi + N_p p + N_{vvv}v^3 + N_{rrr}r^3 + N_{vvr}v^2 r + N_{vrr}vr^2 \\ & + N_{vv\phi}v^2\phi + N_{v\phi\phi}v\phi^2 + N_{rr\phi}r^2\phi + N_{r\phi\phi}r\phi^2 + N_\delta \cos\delta + N_{\text{ext}} \end{aligned} \tag{7.161}$$

where $X(u)$ is usually modeled as quadratic drag $X(u) = X_{|u|u}|u|u$ and the subscript ext denotes external forces and moments due to wind, waves and ocean currents.

Matlab
The models of Son and Nomoto (1981) are implemented in the MSS toolbox as

```
[xdot,U] = container(x,ui)
```

The linearized model for $U = U_0$ is accessed as

```
[xdot,U] = Lcontainer(x,ui,U0)
```

where `x=[u v r x y psi p phi delta]'` and `ui=[delta_c n_c]'`. In the linear case only one input, `delta_c`, is used since the forward speed `U0` is constant. For the nonlinear model, propeller rpm, `n_c`, should be positive.

7.4.2 *The Nonlinear Model of Blanke and Christensen*

An alternative model formulation describing the steering and roll motions of ships has been proposed by Blanke and Christensen (1993). This model is written as

$$\boldsymbol{M}\dot{\boldsymbol{\nu}} + \boldsymbol{C}_{RB}(\boldsymbol{\nu})\boldsymbol{\nu} + \boldsymbol{G}\boldsymbol{\eta} = \boldsymbol{\tau}_{\text{hyd}} + \boldsymbol{\tau}_{\text{wind}} + \boldsymbol{\tau}_{\text{wave}} + \boldsymbol{\tau} \tag{7.162}$$

where $\boldsymbol{\nu} = [v, p, r]^\top$, $\boldsymbol{\tau}_{\text{hyd}} = [Y, K, N]^\top$ and

$$\boldsymbol{M} = \begin{bmatrix} m - Y_{\dot{v}} & -mz_g - Y_{\dot{p}} & mx_g - Y_{\dot{r}} \\ -mz_g - K_{\dot{v}} & I_x - K_{\dot{p}} & 0 \\ mx_g - N_{\dot{v}} & 0 & I_z - N_{\dot{r}} \end{bmatrix} \tag{7.163}$$

$$\boldsymbol{C}_{RB}(\boldsymbol{\nu}) = \begin{bmatrix} 0 & 0 & mu \\ 0 & 0 & 0 \\ -mu & 0 & 0 \end{bmatrix} \tag{7.164}$$

$$\boldsymbol{G} = \begin{bmatrix} 0 & 0 & 0 \\ 0 & -K_\phi & 0 \\ 0 & 0 & 0 \end{bmatrix} \tag{7.165}$$

The hydrodynamic forces in $\boldsymbol{\tau}_{\text{hyd}}$ include both damping and hydrodynamic Coriolis and centripetal terms:

$$\begin{aligned} Y &= Y_{|u|v}|u|v + Y_{ur}ur + Y_{v|v|}|v|v + Y_{v|r|}v|r| + Y_{|v|r}|v|r \\ &\quad + Y_{\phi|uv|}\phi|uv| + Y_{\phi|ur|}\phi|ur| + Y_{\phi uu}\phi u^2 + Y_{\text{ext}} \end{aligned} \tag{7.166}$$

$$\begin{aligned} K &= K_{|u|v}|u|v + K_{ur}ur + K_{v|v|}|v|v + K_{v|r|}v|r| + K_{|v|r}|v|r \\ &\quad + K_{\phi|uv|}\phi|uv| + K_{\phi|ur|}\phi|ur| + K_{\phi uu}\phi u^2 + K_{|u|p}|u|p \\ &\quad + K_{p|p|}p|p| + K_p p + K_{\phi\phi\phi}\phi^3 + K_{\text{ext}} \end{aligned} \tag{7.167}$$

$$\begin{aligned} N &= N_{|u|v}|u|v + N_{|u|r}|u|r + N_{r|r|}|r|r + N_{v|r|}v|r| + N_{|v|r}|v|r \\ &\quad + N_{\phi|uv|}\phi|uv| + N_{\phi|ur|}\phi|ur| + N_p p + N_{|p|p}|p|p + N_{|u|p}|u|p \\ &\quad + N_{\phi u|u|}\phi|u|u| + N_{\text{ext}} \end{aligned} \tag{7.168}$$

where the forces and moments associated with the roll motion are assumed to involve the square terms of the surge speed u^2 and $|u|u$. The terms Y_{ext}, K_{ext} and N_{ext} consist of possible contributions from external disturbances while control inputs such as rudders, propellers and bow thrusters are included in $\boldsymbol{\tau}$.

7.4.3 Nonlinear Model Based on Low-Aspect Ratio Wing Theory

In Ross (2008), the ship is modeled as a low-aspect ratio wing. This approach is well suited to derive a physical *model structure* that can best describe the nonlinear damping forces acting on a marine craft. The parameters of the model must, however, be found by curve fitting the simulated response to time series, for instance by using system identification. In this approach, the lift and drag are derived from two coefficients: namely the lift and drag coefficients, respectively. The resulting expressions are

$$\begin{aligned} X_{LD} &= X^L_{uu}u^2 + X^L_{uuu}u^3 + X^L_{vv}v^2 + X^L_{rr}r^2 + X^L_{rv}rv + X^L_{uvv}uv^2 \\ &\quad + X^L_{rvu}rvu + X^L_{urr}ur^2 + \underbrace{X^L_{vv\phi\phi}v^2\phi^2 + X^L_{vr\phi\phi}vr\phi^2 + X^L_{rr\phi\phi}r^2\phi^2}_{\Delta X_{LD}} \end{aligned} \tag{7.169}$$

$$\begin{aligned} Y_{LD} &= Y^L_{uv}uv + Y^L_{ur}ur + Y^L_{uur}u^2r + Y^L_{uuv}u^2v + Y^L_{vvv}v^3 + Y^L_{rrr}r^3 \\ &\quad + Y^L_{rrv}r^2v + Y^L_{vvr}v^2r + \underbrace{Y^L_{uv\phi\phi}uv\phi^2 + Y^L_{ur\phi\phi}ur\phi^2}_{\Delta Y_{LD}} \end{aligned} \tag{7.170}$$

$$\begin{aligned} K_{LD} &= Y_{LD}z_{cp} \\ &= K^L_{uv}uv + K^L_{ur}ur + K^L_{uur}u^2r + K^L_{uuv}u^2v + K^L_{vvv}v^3 \\ &\quad + K^L_{rrr}r^3 + K^L_{rrv}r^2v + K^L_{vvr}v^2r + K^L_{uv\phi\phi}uv\phi^2 + K^L_{ur\phi\phi}ur\phi^2 \end{aligned} \tag{7.171}$$

$$
\begin{aligned}
N_{LD} &= Y_{LD} x_{cp} \\
&= N^L_{uv} uv + N^L_{ur} ur + N^L_{uur} u^2 r + N^L_{uuv} u^2 v + N^L_{vvv} v^3 \\
&\quad + N^L_{rrr} r^3 + N^L_{rrv} r^2 v + N^L_{vvr} v^2 r + N^L_{uv\phi\phi} uv\phi^2 + N^L_{ur\phi\phi} ur\phi^2
\end{aligned} \tag{7.172}
$$

where (x_{cp}, z_{cp}) defines the location of the center of pressure. The roll angle influence on lift and drag is modeled by

$$
\Delta X_{LD} = X^L_{vv\phi\phi} v^2\phi^2 + X^L_{vr\phi\phi} vr\phi^2 + X^L_{rr\phi\phi} r^2\phi^2 \tag{7.173}
$$

$$
\Delta Y_{LD} = Y^L_{uv\phi\phi} uv\phi^2 + Y^L_{ur\phi\phi} ur\phi^2 \tag{7.174}
$$

In addition to this, viscous roll damping is modeled by a third-order dissipative odd function:

$$
K = -K_p p - K_{ppp} p^3 \tag{7.175}
$$

The lift and drag forces are forces that arise from circulatory effects. However, since the ship hull is being treated as a low-aspect ratio wing, it is necessary to include an additional nonlinear lift component, with an associated induced drag term. The additional nonlinear lift forces are recognized as the cross-flow drag terms:

$$
Y = Y_{|v|v}|v|v + Y_{|v|r}|v|r + Y_{v|r|}v|r| + Y_{|r|r}|r|r| \tag{7.176}
$$

$$
K = K_{|v|v}|v|v + K_{|v|r}|v|r + K_{v|r|}v|r| + K_{|r|r}|r|r| \tag{7.177}
$$

$$
N = N_{|v|v}|v|v + N_{|v|r}|v|r + N_{v|r|}v|r| + N_{|r|r}|r|r| \tag{7.178}
$$

which were derived in Section 6.4.3.

The resulting damping matrix is

$$
\boldsymbol{D}(\boldsymbol{\nu}) =
\begin{bmatrix}
\begin{matrix} -X^L_{uu} u - X^L_{uuu} u^2 \\ -X^L_{ruu} ru \end{matrix} & \begin{matrix} -X^L_{vv} v - X^L_{rv} r \\ -X^L_{uvv} uv - X^L_{vv\phi\phi} v\phi^2 \\ -X^L_{vr\phi\phi} r\phi^2 \end{matrix} & 0 & -X^L_{rr} r - X^L_{urr} ur - X^L_{rr\phi\phi} r\phi^2 \\
\begin{matrix} -Y^L_{uv\phi\phi} v\phi^2 - Y^L_{ur\phi\phi} r\phi^2 \end{matrix} & \begin{matrix} -Y^L_{uv} u - Y^L_{uuv} u^2 - Y^L_{vvv} v^2 \\ -Y^L_{rrv} r^2 - Y_{|v|v}|v| - Y_{v|r|}|r| \end{matrix} & 0 & \begin{matrix} -Y^L_{ur} u - Y^L_{uur} u^2 - Y^L_{rrr} r^2 \\ -Y^L_{vvr} v^2 - Y_{|v|r}|v| - Y_{|r|r}|r| \end{matrix} \\
\begin{matrix} -K^L_{uv\phi\phi} v\phi^2 - K^L_{ur\phi\phi} r\phi^2 \end{matrix} & \begin{matrix} -K^L_{uv} u - K^L_{uuv} u^2 - K^L_{vvv} v^2 \\ -K^L_{rrv} r^2 - K_{|v|v}|v| - K_{v|r|}|r| \end{matrix} & -K_p - K_{ppp} p^2 & \begin{matrix} -K^L_{ur} u - K^L_{uur} u^2 - K^L_{rrr} r^2 \\ -K^L_{vvr} v^2 - K_{|v|r}|v| - K_{|r|r}|r| \end{matrix} \\
\begin{matrix} -N^L_{uv\phi\phi} v\phi^2 - N^L_{ur\phi\phi} r\phi^2 \end{matrix} & \begin{matrix} -N^L_{uv} u - N^L_{uuv} u^2 - N^L_{vvv} v^2 \\ -N^L_{rrv} r^2 - N_{|v|v}|v| - N_{v|r|}|r| \end{matrix} & 0 & \begin{matrix} -N^L_{ur} u - N^L_{uur} u^2 - N^L_{rrr} r^2 \\ -N^L_{vvr} v^2 - N_{|v|r}|v| - N_{|r|r}|r| \end{matrix}
\end{bmatrix} \tag{7.179}
$$

The 4 DOF equations of motion are

$$
\boldsymbol{M}\dot{\boldsymbol{\nu}} + \boldsymbol{C}_{RB}(\boldsymbol{\nu})\boldsymbol{\nu} + \boldsymbol{C}_A(\boldsymbol{\nu})\boldsymbol{\nu} + \boldsymbol{D}(\boldsymbol{\nu})\boldsymbol{\nu} + \boldsymbol{G}\boldsymbol{\eta} = \boldsymbol{\tau} + \boldsymbol{\tau}_{\text{wind}} + \boldsymbol{\tau}_{\text{wave}} \tag{7.180}
$$

where

$$\boldsymbol{M} = \begin{bmatrix} m - X_{\dot{u}} & 0 & 0 & 0 \\ 0 & m - Y_{\dot{v}} & -mz_g - Y_{\dot{p}} & mx_g - Y_{\dot{r}} \\ 0 & -mz_g - K_{\dot{v}} & I_x - K_{\dot{p}} & 0 \\ 0 & mx_g - N_{\dot{v}} & 0 & I_z - N_{\dot{r}} \end{bmatrix} \tag{7.181}$$

$$\boldsymbol{C}_{RB}(\boldsymbol{\nu}) = \begin{bmatrix} 0 & 0 & mz_g r & -m(x_g r + v) \\ 0 & 0 & 0 & mu \\ -mz_g r & 0 & 0 & 0 \\ m(x_g r + v) & -mu & 0 & 0 \end{bmatrix} \tag{7.182}$$

$$\boldsymbol{C}_A(\boldsymbol{\nu}) = \begin{bmatrix} 0 & 0 & 0 & Y_{\dot{v}} v \\ 0 & 0 & 0 & -X_{\dot{u}} u \\ 0 & 0 & 0 & Y_{\dot{v}} v \\ -Y_{\dot{v}} v & X_{\dot{u}} u & -Y_{\dot{v}} v & 0 \end{bmatrix} \tag{7.183}$$

$$\boldsymbol{G} = \begin{bmatrix} 0 & 0 & 0 & 0 \\ 0 & 0 & 0 & 0 \\ 0 & 0 & -K_{\phi} & 0 \\ 0 & 0 & 0 & 0 \end{bmatrix} \tag{7.184}$$

7.5 Equations of Motion (6 DOF)

Ship models are usually reduced-order models for control of the horizontal plane motions (*surge, sway* and *yaw*) in combination with *roll* if roll damping is an issue. Semi-submersible control systems are also designed for the stabilization of the horizontal plane motions, but for these types of vessels it is also of interest to simulate the *heave, roll* and *pitch* motions during critical operations such as drilling. The rolling and pitching of a semi-submersible can also be stabilized by using the thrusters located on the pontoons since these have large moment arms that produce restoring moments. The 3 and 4 DOF models in the previous sections are intended for model-based control and observer design (see Section 1.1).

In this section we will discuss 6 DOF models, which are useful for prediction, simulation and control of marine craft performing coupled motions. A 6 DOF model is usually implemented in a computer to describe all dynamics effects as accurately as possible. This is referred to as the *simulation model*; see Figure 1.4 in Section 1.1. The simulation model should be able to reconstruct the time responses of the physical system. Model-based controllers and observers, however, can be designed using reduced-order or simplified models. For marine craft with actuation in all DOFs, such as underwater vehicles, a model-based controller and observer design requires a 6 DOF model, while ship and semi-submersible control systems can be designed using a 3 or 4 DOF model.

7.5.1 Nonlinear 6 DOF Vector Representations in BODY and NED

When designing feedback control systems it can be advantageous to formulate the equations of motion in both the $\{b\}$ and $\{n\}$ frames in order to exploit physical properties of the model. This section includes nonlinear transformations that can be used to represent the equations of motion in different reference frames.

Equations of Motion Expressed in BODY

Consider the nonlinear equations of motion expressed in $\{b\}$ with $\boldsymbol{v}_c = \boldsymbol{0}$:

$$\dot{\boldsymbol{\eta}} = \boldsymbol{J}_k(\boldsymbol{\eta})\boldsymbol{\nu} \tag{7.185}$$

$$\boldsymbol{M}\dot{\boldsymbol{\nu}} + \boldsymbol{C}(\boldsymbol{\nu})\boldsymbol{\nu} + \boldsymbol{D}(\boldsymbol{\nu})\boldsymbol{\nu} + \boldsymbol{g}(\boldsymbol{\eta}) + \boldsymbol{g}_o = \boldsymbol{\tau} + \boldsymbol{\tau}_{\text{wind}} + \boldsymbol{\tau}_{\text{wave}} \tag{7.186}$$

where

$$\boldsymbol{M} = \boldsymbol{M}_{RB} + \boldsymbol{M}_A \tag{7.187}$$

$$\boldsymbol{C}(\boldsymbol{\nu}) = \boldsymbol{C}_{RB}(\boldsymbol{\nu}) + \boldsymbol{C}_A(\boldsymbol{\nu}) \tag{7.188}$$

$$\boldsymbol{D}(\boldsymbol{\nu}) = \boldsymbol{D} + \boldsymbol{D}_n(\boldsymbol{\nu}) \tag{7.189}$$

The expressions for $\boldsymbol{\eta}$ and $\boldsymbol{J}_k(\boldsymbol{\eta})$ depend on the kinematic representation. Three different choices for $\boldsymbol{J}_k(\boldsymbol{\eta})$ will be presented where the subscript $k \in \{\Theta, q, r\}$ denotes the Euler angle, quaternion and rotation matrix representation, respectively.

Equations of Motion Expressed in NED

The equations of motion (7.186) when transformed to $\{n\}$ take the following form:

$$\boldsymbol{M}^*(\boldsymbol{\eta})\ddot{\boldsymbol{\eta}} + \boldsymbol{C}^*(\boldsymbol{\nu}, \boldsymbol{\eta})\dot{\boldsymbol{\eta}} + \boldsymbol{D}^*(\boldsymbol{\nu}, \boldsymbol{\eta})\dot{\boldsymbol{\eta}} + \boldsymbol{g}^*(\boldsymbol{\eta}) + \boldsymbol{g}_o^*(\boldsymbol{\eta}) = \boldsymbol{\tau}^* + \boldsymbol{\tau}_{\text{wind}}^* + \boldsymbol{\tau}_{\text{wave}}^* \tag{7.190}$$

where the expressions for $\boldsymbol{M}^*$, $\boldsymbol{C}^*(\boldsymbol{\nu}, \boldsymbol{\eta})$, $\boldsymbol{D}^*(\boldsymbol{\nu}, \boldsymbol{\eta})$, $\boldsymbol{g}^*(\boldsymbol{\eta})$, $\boldsymbol{g}_o^*(\boldsymbol{\eta})$, $\boldsymbol{\tau}^*$, $\boldsymbol{\tau}_{\text{wind}}^*$, $\boldsymbol{\tau}_{\text{wave}}^*$ and the associated kinematic transformations depend on how attitude is represented. Three different choices are outlined below:

1. **Positions and Euler Angles ($\boldsymbol{k} = \boldsymbol{\Theta}$):** The Euler angle representation (2.40) is based on the three parameters ϕ, θ and ψ. This gives

$$\boldsymbol{J}_\Theta(\boldsymbol{\eta}) := \begin{bmatrix} \boldsymbol{R}_b^n(\boldsymbol{\Theta}_{nb}) & \boldsymbol{0}_{3\times3} \\ \boldsymbol{0}_{3\times3} & \boldsymbol{T}_\Theta(\boldsymbol{\Theta}_{nb}) \end{bmatrix}, \quad \boldsymbol{J}_\Theta^{-1}(\boldsymbol{\eta}) = \begin{bmatrix} \boldsymbol{R}_b^n(\boldsymbol{\Theta}_{nb})^\top & \boldsymbol{0}_{3\times3} \\ \boldsymbol{0}_{3\times3} & \boldsymbol{T}_\Theta^{-1}(\boldsymbol{\Theta}_{nb}) \end{bmatrix} \tag{7.191}$$

   where $\boldsymbol{\eta} := [N, E, D, \phi, \theta, \psi]^\top$. The representation singularity at $\theta \neq \pm\pi/2$ in the expression for $\boldsymbol{T}_\Theta$ implies that the inverse matrix $\boldsymbol{J}_\Theta^{-1}(\boldsymbol{\eta})$ does not exist at this value. The transformation is as follows:

$$\begin{aligned} \dot{\boldsymbol{\eta}} &= \boldsymbol{J}_\Theta(\boldsymbol{\eta})\boldsymbol{\nu} \quad &\Longleftrightarrow \quad \boldsymbol{\nu} &= \boldsymbol{J}_\Theta^{-1}(\boldsymbol{\eta})\dot{\boldsymbol{\eta}} \\ \ddot{\boldsymbol{\eta}} &= \boldsymbol{J}_\Theta(\boldsymbol{\eta})\dot{\boldsymbol{\nu}} + \dot{\boldsymbol{J}}_\Theta(\boldsymbol{\eta})\boldsymbol{\nu} \quad &\Longleftrightarrow \quad \dot{\boldsymbol{\nu}} &= \boldsymbol{J}_\Theta^{-1}(\boldsymbol{\eta})[\ddot{\boldsymbol{\eta}} - \dot{\boldsymbol{J}}_\Theta(\boldsymbol{\eta})\boldsymbol{J}_\Theta^{-1}(\boldsymbol{\eta})\dot{\boldsymbol{\eta}}] \end{aligned}$$

and

$$\begin{aligned}
\boldsymbol{M}^*(\boldsymbol{\eta}) &= \boldsymbol{J}_\Theta^{-\top}(\boldsymbol{\eta})\boldsymbol{M}\boldsymbol{J}_\Theta^{-1}(\boldsymbol{\eta}) \\
\boldsymbol{C}^*(\boldsymbol{\nu},\boldsymbol{\eta}) &= \boldsymbol{J}_\Theta^{-\top}(\boldsymbol{\eta})[\boldsymbol{C}(\boldsymbol{\nu}) - \boldsymbol{M}\boldsymbol{J}_\Theta^{-1}(\boldsymbol{\eta})\dot{\boldsymbol{J}}_\Theta(\boldsymbol{\eta})]\boldsymbol{J}_\Theta^{-1}(\boldsymbol{\eta}) \\
\boldsymbol{D}^*(\boldsymbol{\nu},\boldsymbol{\eta}) &= \boldsymbol{J}_\Theta^{-\top}(\boldsymbol{\eta})\boldsymbol{D}(\boldsymbol{\nu})\boldsymbol{J}_\Theta^{-1}(\boldsymbol{\eta}) \\
\boldsymbol{g}^*(\boldsymbol{\eta}) + \boldsymbol{g}_o^*(\boldsymbol{\eta}) &= \boldsymbol{J}_\Theta^{-\top}(\boldsymbol{\eta})[\boldsymbol{g}(\boldsymbol{\eta}) + \boldsymbol{g}_o] \\
\boldsymbol{\tau}^* + \boldsymbol{\tau}_{\text{wind}}^* + \boldsymbol{\tau}_{\text{wave}}^* &= \boldsymbol{J}_\Theta^{-\top}(\boldsymbol{\eta})(\boldsymbol{\tau} + \boldsymbol{\tau}_{\text{wind}} + \boldsymbol{\tau}_{\text{wave}})
\end{aligned} \tag{7.192}$$

2. Positions and Quaternions ($\boldsymbol{k} = \boldsymbol{q}$): The quaternion representation (2.69) avoids the singular points $\theta \neq \pm\pi/2$ by using four parameters (unit quaternions) η, ε_1, ε_2 and ε_3 to represent attitude:

$$\boldsymbol{J}_q(\boldsymbol{\eta}) := \begin{bmatrix} \boldsymbol{R}_b^n(\boldsymbol{q}) & \boldsymbol{0}_{3\times 3} \\ \boldsymbol{0}_{4\times 3} & \boldsymbol{T}_q(\boldsymbol{q}) \end{bmatrix}, \qquad \boldsymbol{J}_q^\dagger(\boldsymbol{\eta}) = \begin{bmatrix} \boldsymbol{R}_b^n(\boldsymbol{q})^\top & \boldsymbol{0}_{3\times 4} \\ \boldsymbol{0}_{4\times 3} & 4\boldsymbol{T}_q^\top(\boldsymbol{q}) \end{bmatrix} \tag{7.193}$$

Notice that pseudo-inverse $\boldsymbol{J}_q^\dagger(\boldsymbol{\eta})$ is computed using the left *Moore–Penrose pseudo-inverse* and by exploiting the property $\boldsymbol{T}_q^\top(\boldsymbol{q})\boldsymbol{T}_q(\boldsymbol{q}) = 1/4\boldsymbol{I}_{3\times 3}$. Moreover, the left inverse of $\boldsymbol{T}_q(\boldsymbol{q})$ is

$$\begin{aligned}
\boldsymbol{T}_q^\dagger(\boldsymbol{q}) &= \left(\boldsymbol{T}_q^\top(\boldsymbol{q})\boldsymbol{T}_q(\boldsymbol{q})\right)^{-1}\boldsymbol{T}_q^\top(\boldsymbol{q}) \\
&= 4\boldsymbol{T}_q^\top(\boldsymbol{q})
\end{aligned} \tag{7.194}$$

For this case, $\boldsymbol{\eta} := [N, E, D, \eta, \varepsilon_1, \varepsilon_1, \varepsilon_1]^\top$ and

$$\begin{aligned}
\dot{\boldsymbol{\eta}} &= \boldsymbol{J}_q(\boldsymbol{\eta})\boldsymbol{\nu} &&\iff \quad \boldsymbol{\nu} = \boldsymbol{J}_q^\dagger(\boldsymbol{\eta})\dot{\boldsymbol{\eta}} \\
\ddot{\boldsymbol{\eta}} &= \boldsymbol{J}_q(\boldsymbol{\eta})\dot{\boldsymbol{\nu}} + \dot{\boldsymbol{J}}_q(\boldsymbol{\eta})\boldsymbol{\nu} &&\iff \quad \dot{\boldsymbol{\nu}} = \boldsymbol{J}_q^\dagger(\boldsymbol{\eta})[\ddot{\boldsymbol{\eta}} - \dot{\boldsymbol{J}}_q(\boldsymbol{\eta})\boldsymbol{J}_q^\dagger(\boldsymbol{\eta})\dot{\boldsymbol{\eta}}]
\end{aligned}$$

and

$$\begin{aligned}
\boldsymbol{M}^*(\boldsymbol{\eta}) &= \boldsymbol{J}_q^\dagger(\boldsymbol{\eta})^\top\boldsymbol{M}\boldsymbol{J}_q^\dagger(\boldsymbol{\eta}) \\
\boldsymbol{C}^*(\boldsymbol{\nu},\boldsymbol{\eta}) &= \boldsymbol{J}_q^\dagger(\boldsymbol{\eta})^\top[\boldsymbol{C}(\boldsymbol{\nu}) - \boldsymbol{M}\boldsymbol{J}_q^\dagger(\boldsymbol{\eta})\dot{\boldsymbol{J}}_q(\boldsymbol{\eta})]\boldsymbol{J}_q^\dagger(\boldsymbol{\eta}) \\
\boldsymbol{D}^*(\boldsymbol{\nu},\boldsymbol{\eta}) &= \boldsymbol{J}_q^\dagger(\boldsymbol{\eta})^\top\boldsymbol{D}(\boldsymbol{\nu})\boldsymbol{J}_q^\dagger(\boldsymbol{\eta}) \\
\boldsymbol{g}^*(\boldsymbol{\eta}) + \boldsymbol{g}_o^*(\boldsymbol{\eta}) &= \boldsymbol{J}_q^\dagger(\boldsymbol{\eta})^\top[\boldsymbol{g}(\boldsymbol{\eta}) + \boldsymbol{g}_o] \\
\boldsymbol{\tau}^* + \boldsymbol{\tau}_{\text{wind}}^* + \boldsymbol{\tau}_{\text{wave}}^* &= \boldsymbol{J}_q^\dagger(\boldsymbol{\eta})^\top(\boldsymbol{\tau} + \boldsymbol{\tau}_{\text{wind}} + \boldsymbol{\tau}_{\text{wave}})
\end{aligned} \tag{7.195}$$

3. Positions and Angular Rates ($\boldsymbol{k} = \boldsymbol{r}$): A singularity free three-parameter transformation based on the rotation matrix $\boldsymbol{R}_b^n(\boldsymbol{\Theta}_{nb})$ and its inverse $\boldsymbol{R}_b^n(\boldsymbol{\Theta}_{nb})^{-1} = \boldsymbol{R}_b^n(\boldsymbol{\Theta}_{nb})^\top$ is

$$\boldsymbol{J}_r(\boldsymbol{\eta}) := \begin{bmatrix} \boldsymbol{R}_b^n(\boldsymbol{\Theta}_{nb}) & \boldsymbol{0}_{3\times 3} \\ \boldsymbol{0}_{3\times 3} & \boldsymbol{R}_b^n(\boldsymbol{\Theta}_{nb}) \end{bmatrix}, \quad \boldsymbol{J}_r^{-1}(\boldsymbol{\eta}) = \boldsymbol{J}_r^\top(\boldsymbol{\eta}) \tag{7.196}$$

where the last three states are angular rates expressed in $\{n\}$. This gives

$$\begin{aligned}
\dot{\boldsymbol{\eta}} &= \boldsymbol{J}_r(\boldsymbol{\eta})\boldsymbol{\nu} &&\iff \quad \boldsymbol{\nu} = \boldsymbol{J}_r^\top(\boldsymbol{\eta})\dot{\boldsymbol{\eta}} \\
\ddot{\boldsymbol{\eta}} &= \boldsymbol{J}_r(\boldsymbol{\eta})\dot{\boldsymbol{\nu}} + \dot{\boldsymbol{J}}_r(\boldsymbol{\eta})\boldsymbol{\nu} &&\iff \quad \dot{\boldsymbol{\nu}} = \boldsymbol{J}_r^\top(\boldsymbol{\eta})\left[\ddot{\boldsymbol{\eta}} - \dot{\boldsymbol{J}}_r(\boldsymbol{\eta})\boldsymbol{J}_r^\top(\boldsymbol{\eta})\dot{\boldsymbol{\eta}}\right]
\end{aligned}$$

and

$$\begin{aligned}
\boldsymbol{M}^*(\boldsymbol{\eta}) &= \boldsymbol{J}_r(\boldsymbol{\eta})\boldsymbol{M}\boldsymbol{J}_r^\top(\boldsymbol{\eta}) \\
\boldsymbol{C}^*(\boldsymbol{\nu},\boldsymbol{\eta}) &= \boldsymbol{J}_r(\boldsymbol{\eta})[\boldsymbol{C}(\boldsymbol{\nu}) - \boldsymbol{M}\boldsymbol{J}_r(\boldsymbol{\eta})\dot{\boldsymbol{J}}_r(\boldsymbol{\eta})]\boldsymbol{J}_r^\top(\boldsymbol{\eta}) \\
\boldsymbol{D}^*(\boldsymbol{\nu},\boldsymbol{\eta}) &= \boldsymbol{J}_r(\boldsymbol{\eta})\boldsymbol{D}(\boldsymbol{\nu})\boldsymbol{J}_r^\top(\boldsymbol{\eta}) \\
\boldsymbol{g}^*(\boldsymbol{\eta}) + \boldsymbol{g}_o^*(\boldsymbol{\eta}) &= \boldsymbol{J}_r(\boldsymbol{\eta})[\boldsymbol{g}(\boldsymbol{\eta}) + \boldsymbol{g}_o] \\
\boldsymbol{\tau}^* + \boldsymbol{\tau}^*_{\text{wind}} + \boldsymbol{\tau}^*_{\text{wave}} &= \boldsymbol{J}_r(\boldsymbol{\eta})(\boldsymbol{\tau} + \boldsymbol{\tau}_{\text{wind}} + \boldsymbol{\tau}_{\text{wave}})
\end{aligned} \tag{7.197}$$

The following properties hold for the body-fixed vector representation:

Property 7.1 (System Inertia Matrix M)
For a rigid body the system inertia matrix is positive definite and constant, that is

$$\boldsymbol{M} = \boldsymbol{M}^\top > 0, \quad \dot{\boldsymbol{M}} = \boldsymbol{0}$$

where $\boldsymbol{M}$ *is defined as*

$$\boldsymbol{M} := \begin{bmatrix}
m - X_{\dot{u}} & -X_{\dot{v}} & -X_{\dot{w}} & -X_{\dot{p}} & mz_g - X_{\dot{q}} & -my_g - X_{\dot{r}} \\
-X_{\dot{v}} & m - Y_{\dot{v}} & -Y_{\dot{w}} & -mz_g - Y_{\dot{p}} & -Y_{\dot{q}} & mx_g - Y_{\dot{r}} \\
-X_{\dot{w}} & -Y_{\dot{w}} & m - Z_{\dot{w}} & my_g - Z_{\dot{p}} & -mx_g - Z_{\dot{q}} & -Z_{\dot{r}} \\
-X_{\dot{p}} & -mz_g - Y_{\dot{p}} & my_g - Z_{\dot{p}} & I_x - K_{\dot{p}} & -I_{xy} - K_{\dot{q}} & -I_{zx} - K_{\dot{r}} \\
mz_g - X_{\dot{q}} & -Y_{\dot{q}} & -mx_g - Z_{\dot{q}} & -I_{xy} - K_{\dot{q}} & I_y - M_{\dot{q}} & -I_{yz} - M_{\dot{r}} \\
-my_g - X_{\dot{r}} & mx_g - Y_{\dot{r}} & -Z_{\dot{r}} & -I_{zx} - K_{\dot{r}} & -I_{yz} - M_{\dot{r}} & I_z - N_{\dot{r}}
\end{bmatrix}$$

Property 7.2 (Coriolis and Centripetal Matrix C)
For a rigid body moving through an ideal fluid the Coriolis and centripetal matrix $\boldsymbol{C}(\boldsymbol{\nu})$ *can always be parameterized such that it is skew-symmetric, that is*

$$\boldsymbol{C}(\boldsymbol{\nu}) = -\boldsymbol{C}^\top(\boldsymbol{\nu}), \quad \forall \boldsymbol{\nu} \in \mathbb{R}^6$$

Proof. $\boldsymbol{C}(\boldsymbol{\nu})$ is skew-symmetric under the assumptions that the matrices $\boldsymbol{C}_{RB}(\boldsymbol{\nu})$ and $\boldsymbol{C}_A(\boldsymbol{\nu})$ are skew-symmetric.

For the vector representation in $\{n\}$ it is straightforward to show that:

1. $\boldsymbol{M}^*(\boldsymbol{\eta}) = \boldsymbol{M}^*(\boldsymbol{\eta})^\top > 0$
2. $\boldsymbol{s}^\top[\dot{\boldsymbol{M}}^*(\boldsymbol{\eta}) - 2\boldsymbol{C}^*(\boldsymbol{\nu},\boldsymbol{\eta})]\boldsymbol{s} = 0$
3. $\boldsymbol{D}^*(\boldsymbol{\nu},\boldsymbol{\eta}) > 0$

since $\boldsymbol{M} = \boldsymbol{M}^\top > 0$ and $\dot{\boldsymbol{M}} = \boldsymbol{0}$. It should be noted that $\boldsymbol{C}^*(\boldsymbol{\nu}, \boldsymbol{\eta})$ will not be skew-symmetrical although $\boldsymbol{C}(\boldsymbol{\nu})$ is skew-symmetrical.

Example 7.8 (Lyapunov Analysis exploiting MIMO Model Properties)
Consider the following model:

$$\dot{\boldsymbol{\eta}} = \boldsymbol{J}_k(\boldsymbol{\eta})\boldsymbol{\nu} \tag{7.198}$$

$$\boldsymbol{M}\dot{\boldsymbol{\nu}} + \boldsymbol{C}(\boldsymbol{\nu})\boldsymbol{\nu} + \boldsymbol{D}(\boldsymbol{\nu})\boldsymbol{\nu} + \boldsymbol{g}(\boldsymbol{\eta}) = \boldsymbol{\tau} \tag{7.199}$$

where $\boldsymbol{J}_k(\boldsymbol{\eta})$ can be represented by $\boldsymbol{J}_\Theta(\boldsymbol{\eta})$, $\boldsymbol{J}_q(\boldsymbol{\eta})$ or $\boldsymbol{J}_r(\boldsymbol{\eta})$. The obvious Lyapunov function candidate is based on kinetic and potential energy:

$$V = \frac{1}{2}\boldsymbol{\nu}^\top \boldsymbol{M}\boldsymbol{\nu} + \frac{1}{2}\boldsymbol{\eta}^\top \boldsymbol{K}_p\boldsymbol{\eta} \tag{7.200}$$

where $\boldsymbol{K}_p = \boldsymbol{K}_p^\top > 0$ is a constant gain matrix. Since $\boldsymbol{M} = \boldsymbol{M}^\top > 0$ and $\dot{\boldsymbol{M}} = \boldsymbol{0}$, it follows that

$$\begin{aligned}\dot{V} &= \boldsymbol{\nu}^\top \boldsymbol{M}\dot{\boldsymbol{\nu}} + \boldsymbol{\eta}^\top \boldsymbol{K}_p\dot{\boldsymbol{\eta}} \\ &= \boldsymbol{\nu}^\top \boldsymbol{M}\dot{\boldsymbol{\nu}} + \boldsymbol{\eta}^\top \boldsymbol{K}_p\boldsymbol{J}_k(\boldsymbol{\eta})\boldsymbol{\nu} \\ &= \boldsymbol{\nu}^\top [\boldsymbol{M}\dot{\boldsymbol{\nu}} + \boldsymbol{J}_k^\top(\boldsymbol{\eta})\boldsymbol{K}_p\boldsymbol{\eta}]\end{aligned} \tag{7.201}$$

Substituting (7.199) into the expression for $\dot{V}$ gives

$$\dot{V} = \boldsymbol{\nu}^\top [\boldsymbol{\tau} - \boldsymbol{C}(\boldsymbol{\nu})\boldsymbol{\nu} - \boldsymbol{D}(\boldsymbol{\nu})\boldsymbol{\nu} - \boldsymbol{g}(\boldsymbol{\eta}) + \boldsymbol{J}_k^\top(\boldsymbol{\eta})\boldsymbol{K}_p\boldsymbol{\eta}] \tag{7.202}$$

Since $\boldsymbol{\nu}^\top \boldsymbol{C}(\boldsymbol{\nu})\boldsymbol{\nu} \equiv \boldsymbol{0}$ and $\boldsymbol{\nu}^\top \boldsymbol{D}(\boldsymbol{\nu})\boldsymbol{\nu} > 0$, we can choose the control law of PD type according to

$$\boldsymbol{\tau} = \boldsymbol{g}(\boldsymbol{\eta}) - \boldsymbol{K}_d\boldsymbol{\nu} - \boldsymbol{J}_k^\top(\boldsymbol{\eta})\boldsymbol{K}_p\boldsymbol{\eta} \tag{7.203}$$

with $\boldsymbol{K}_d > 0$ such that

$$\begin{aligned}\dot{V} &= -\boldsymbol{\nu}^\top [\boldsymbol{K}_d + \boldsymbol{D}(\boldsymbol{\nu})]\boldsymbol{\nu} \\ &\leq 0\end{aligned} \tag{7.204}$$

Consequently, GAS follows from Krasowskii–LaSalle's theorem if $\boldsymbol{J}_k(\boldsymbol{\eta})$ is nonsingular (see Appendix A.1).

7.5.2 Symmetry Considerations of the System Inertia Matrix

We have seen that the 6 DOF nonlinear equations of motion, in their most general representation, require that a large number of hydrodynamic derivatives are known. From a practical point of view this is an unsatisfactory situation. However, the number of unknown parameters can be drastically reduced by using body symmetry conditions.

In general $\boldsymbol{M}_A$ and $\boldsymbol{M}_{RB}$ will be a full matrices in CO. Let

$$\boldsymbol{M} = \boldsymbol{M}_{RB} + \boldsymbol{M}_A, \quad \boldsymbol{M} = \boldsymbol{M}^\top > 0$$

From the definitions of $\boldsymbol{M}_A$ and $\boldsymbol{M}_{RB}$ it is straightforward to verify the following cases (notice that $m_{ij} = m_{ji}$):

(i) xy plane of symmetry (bottom/top symmetry):

$$\boldsymbol{M} = \begin{bmatrix} m_{11} & m_{12} & 0 & 0 & 0 & m_{16} \\ m_{21} & m_{22} & 0 & 0 & 0 & m_{26} \\ 0 & 0 & m_{33} & m_{34} & m_{35} & 0 \\ 0 & 0 & m_{43} & m_{44} & m_{45} & 0 \\ 0 & 0 & m_{53} & m_{54} & m_{55} & 0 \\ m_{61} & m_{62} & 0 & 0 & 0 & m_{66} \end{bmatrix}$$

(ii) xz plane of symmetry (port/starboard symmetry):

$$\boldsymbol{M} = \begin{bmatrix} m_{11} & 0 & m_{13} & 0 & m_{15} & 0 \\ 0 & m_{22} & 0 & m_{24} & 0 & m_{26} \\ m_{31} & 0 & m_{33} & 0 & m_{35} & 0 \\ 0 & m_{42} & 0 & m_{44} & 0 & m_{46} \\ m_{51} & 0 & m_{53} & 0 & m_{55} & 0 \\ 0 & m_{62} & 0 & m_{64} & 0 & m_{66} \end{bmatrix}$$

(iii) yz plane of symmetry (fore/aft symmetry):

$$\boldsymbol{M} = \begin{bmatrix} m_{11} & 0 & 0 & 0 & m_{15} & m_{16} \\ 0 & m_{22} & m_{23} & m_{24} & 0 & 0 \\ 0 & m_{32} & m_{33} & m_{34} & 0 & 0 \\ 0 & m_{42} & m_{43} & m_{44} & 0 & 0 \\ m_{51} & 0 & 0 & 0 & m_{55} & m_{56} \\ m_{61} & 0 & 0 & 0 & m_{65} & m_{66} \end{bmatrix}$$

(iv) xz and yz planes of symmetry (port/starboard and fore/aft symmetries):

$$\boldsymbol{M} = \begin{bmatrix} m_{11} & 0 & 0 & 0 & m_{15} & 0 \\ 0 & m_{22} & 0 & m_{24} & 0 & 0 \\ 0 & 0 & m_{33} & 0 & 0 & 0 \\ 0 & m_{42} & 0 & m_{44} & 0 & 0 \\ m_{51} & 0 & 0 & 0 & m_{55} & 0 \\ 0 & 0 & 0 & 0 & 0 & m_{66} \end{bmatrix}$$

More generally, the resulting inertia matrix for a body with ij and jk planes of symmetry is formed by the intersection $M_{ij \cap jk} = M_{ij} \cap M_{jk}$.

(v) xz, yz and xy planes of symmetry (port/starboard, fore/aft and bottom/top symmetries):

$$\boldsymbol{M} = \text{diag}\{m_{11}, m_{22}, m_{33}, m_{44}, m_{55}, m_{66}\}$$

7.5.3 Linearized Equations of Motion (Vessel Parallel Coordinates)

The following assumption will be applied when deriving the linearized equations of motion:

Assumption 7.1 (Small Roll and Pitch Angles)
The roll and pitch angles

$$\phi, \theta \text{ are small} \tag{7.205}$$

These are good assumptions for marine craft where the pitch and roll motions are limited, that is highly metacentric stable craft.

Vessel Parallel Coordinate System

When deriving the linearized equations of motion it is convenient to introduce a vessel parallel coordinate system obtained by rotating the body axes an angle ψ about the z axis at each time step. Assumption 7.1 implies that

$$\dot{\boldsymbol{\eta}} = \boldsymbol{J}_{\Theta}(\boldsymbol{\eta})\boldsymbol{\nu} \overset{\phi=\theta=0}{\approx} \boldsymbol{P}(\psi)\boldsymbol{\nu} \tag{7.206}$$

where

$$\boldsymbol{P}(\psi) = \begin{bmatrix} \boldsymbol{R}(\psi) & \boldsymbol{0}_{3\times 3} \\ \boldsymbol{0}_{3\times 3} & \boldsymbol{I}_{3\times 3} \end{bmatrix} \tag{7.207}$$

and $\boldsymbol{R}(\psi) = \boldsymbol{R}_{z,\psi}$ is the rotation matrix in yaw.

Definition 7.2 (Vessel Parallel Coordinate System)
The vessel parallel (VP) coordinate system is defined as

$$\boldsymbol{\eta}_p := \boldsymbol{P}^{\top}(\psi)\boldsymbol{\eta} \tag{7.208}$$

where $\boldsymbol{\eta}_p$ is the NED position and attitude vector expressed in $\{b\}$ and $\boldsymbol{P}(\psi)$ is given by (7.207). Notice that $\boldsymbol{P}^{\top}(\psi)\boldsymbol{P}(\psi) = \boldsymbol{I}_{6\times 6}$.

Low-Speed Applications (Stationkeeping)

It is convenient to express the kinematic equations of motion in VP coordinates when using linear theory. From Definition 7.2 it is seen that

$$\begin{aligned} \dot{\boldsymbol{\eta}}_p &= \dot{\boldsymbol{P}}^{\top}(\psi)\boldsymbol{\eta} + \boldsymbol{P}^{\top}(\psi)\dot{\boldsymbol{\eta}} \\ &= \dot{\boldsymbol{P}}^{\top}(\psi)\boldsymbol{P}(\psi)\boldsymbol{\eta}_p + \boldsymbol{P}^{\top}(\psi)\boldsymbol{P}(\psi)\boldsymbol{\nu} \\ &= r\boldsymbol{S}\boldsymbol{\eta}_p + \boldsymbol{\nu} \end{aligned} \tag{7.209}$$

where $r = \dot{\psi}$ and

$$\boldsymbol{S} = \begin{bmatrix} 0 & 1 & 0 & 0 & 0 & 0 \\ -1 & 0 & 0 & 0 & 0 & 0 \\ 0 & 0 & 0 & 0 & 0 & 0 \\ 0 & 0 & 0 & 0 & 0 & 0 \\ 0 & 0 & 0 & 0 & 0 & 0 \end{bmatrix} \tag{7.210}$$

For low-speed applications $r \approx 0$. Hence, (7.209) reduces to six pure integrators:

$$\dot{\boldsymbol{\eta}}_p \approx \boldsymbol{\nu} \tag{7.211}$$

This model is useful since it is linear in $\boldsymbol{\nu}$. In fact, this is the main idea for using VP coordinates in ship and rig control designs.

The gravitational and buoyancy forces can also be expressed in terms of VP coordinates. For small angles ϕ and θ it is seen that (see Section 4.1)

$$\boldsymbol{g}(\boldsymbol{\eta}) \overset{\phi=\theta=0}{\approx} \boldsymbol{P}^{\top}(\psi)\boldsymbol{G}\boldsymbol{\eta} = \underbrace{\boldsymbol{P}^{\top}(\psi)\boldsymbol{G}\boldsymbol{P}(\psi)}_{\boldsymbol{G}}\boldsymbol{\eta}_p = \boldsymbol{G}\boldsymbol{\eta}_p \tag{7.212}$$

Notice that this formula confirms that the restoring forces of a leveled floating vessel ($\phi = \theta = 0$) are independent of the yaw angle ψ. This is illustrated by the following two examples:

Neutrally Buoyant Submersible: For a neutrally buoyant submersible ($W = B$) with $x_g = x_b$ and $y_g = y_b$, Assumption 7.1 implies that (see (4.10))

$$\boldsymbol{G} = \text{diag}\{0, 0, 0, 0, (z_g - z_b)W, (z_g - z_b)W, 0\} \tag{7.213}$$

which is independent of the yaw angle ψ. Hence, (7.213) satisfies (7.212).

Surface Vessel: For a surface vessel, $\boldsymbol{G}$ is defined by (4.26). Thanks to the special structure of

$$\boldsymbol{G} = \begin{bmatrix} \boldsymbol{0}_{2\times 2} & \boldsymbol{0}_{2\times 3} & \begin{matrix} 0 \\ 0 \\ 0 \\ 0 \end{matrix} \\ \boldsymbol{0}_{3\times 2} & \boldsymbol{G}^{\{3,4,5\}} & \\ \begin{matrix} 0 & 0 \end{matrix} & \begin{matrix} 0 & 0 & 0 \end{matrix} & \begin{matrix} 0 \end{matrix} \end{bmatrix}, \quad \boldsymbol{G}^{\{3,4,5\}} = \begin{bmatrix} -Z_z & 0 & -Z_\theta \\ 0 & -K_\phi & 0 \\ -M_z & 0 & -M_\theta \end{bmatrix} \tag{7.214}$$

it is again seen that $\boldsymbol{P}^{\top}(\psi)\boldsymbol{G}\boldsymbol{P}(\psi) \equiv \boldsymbol{G}$.

Assumption 7.1 for low-speed applications $\boldsymbol{\nu} \approx \boldsymbol{0}$ implies that the nonlinear Coriolis, centripetal, damping, restoring and buoyancy forces and moments can be linearized about $\boldsymbol{\nu} = \boldsymbol{0}$ and $\phi = \theta = 0$.

Since $\boldsymbol{C}(\boldsymbol{0}) = \boldsymbol{0}$ and $\boldsymbol{D}_n(\boldsymbol{0}) = \boldsymbol{0}$ it makes sense to approximate

$$\boldsymbol{M}\dot{\boldsymbol{\nu}} + \underbrace{\boldsymbol{C}(\boldsymbol{\nu})\boldsymbol{\nu}}_{\boldsymbol{0}} + \underbrace{[\boldsymbol{D} + \boldsymbol{D}_n(\boldsymbol{\nu})]\boldsymbol{\nu}}_{\boldsymbol{D}\boldsymbol{\nu}} + \underbrace{\boldsymbol{g}(\boldsymbol{\eta})}_{\boldsymbol{G}\boldsymbol{\eta}_p} + \boldsymbol{g}_o = \boldsymbol{\tau} + \underbrace{\boldsymbol{\tau}_{\text{wind}} + \boldsymbol{\tau}_{\text{wave}}}_{\boldsymbol{w}} \tag{7.215}$$

which for $\boldsymbol{g}_o = \boldsymbol{0}$ gives

$$\dot{\boldsymbol{\eta}}_p = \boldsymbol{\nu} \tag{7.216}$$

$$\boldsymbol{M}\dot{\boldsymbol{\nu}} + \boldsymbol{D}\boldsymbol{\nu} + \boldsymbol{G}\boldsymbol{\eta}_p = \boldsymbol{\tau} + \boldsymbol{w} \tag{7.217}$$

This is a linear time-invariant (LTI) state-space model

$$\dot{\boldsymbol{x}} = \boldsymbol{A}\boldsymbol{x} + \boldsymbol{B}\boldsymbol{u} + \boldsymbol{E}\boldsymbol{w} \tag{7.218}$$

where $\boldsymbol{x} = [\boldsymbol{\eta}_p^\top, \boldsymbol{\nu}^\top]^\top$, $\boldsymbol{u} = \boldsymbol{\tau}$ and

$$\boldsymbol{A} = \begin{bmatrix} \boldsymbol{0} & \boldsymbol{I} \\ -\boldsymbol{M}^{-1}\boldsymbol{G} & -\boldsymbol{M}^{-1}\boldsymbol{D} \end{bmatrix}, \quad \boldsymbol{B} = \begin{bmatrix} \boldsymbol{0} \\ \boldsymbol{M}^{-1} \end{bmatrix}, \quad \boldsymbol{E} = \begin{bmatrix} \boldsymbol{0} \\ \boldsymbol{M}^{-1} \end{bmatrix} \tag{7.219}$$

The model (7.216)–(7.217) is the foundation for DP and PM control systems design (see Figure 7.9). A linear optimal controller based on (7.216)–(7.217) is presented in Section 13.1.6 while optimal state estimation is discussed in Section 11.3.6.

Notice that the NED positions are computed from $\boldsymbol{\eta}_p$ by using:

$$\boldsymbol{\eta} = \boldsymbol{P}(\psi)\boldsymbol{\eta}_p \tag{7.220}$$

Hence, the control system can be based on feedback from the states $(\boldsymbol{\eta}_p, \boldsymbol{\nu})$ while $\boldsymbol{\eta}$ is presented to the human operator using (7.220).

Marine Craft in Transit (Cruise Condition)

For marine craft in transit the cruise speed is assumed to satisfy

$$u = u_o \tag{7.221}$$

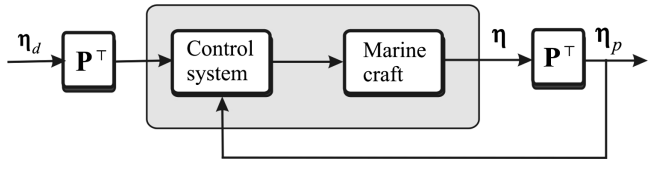

Figure 7.9 Transformation of desired position $\boldsymbol{\eta}_d$ and measured position $\boldsymbol{\eta}$ in a feedback control system using vessel parallel coordinates.

This suggests that

$$\boldsymbol{N}(u_o) = \frac{\partial}{\partial \boldsymbol{\nu}} \left\{ \boldsymbol{C}(\boldsymbol{\nu})\boldsymbol{\nu} + \boldsymbol{D}(\boldsymbol{\nu})\boldsymbol{\nu} \right\}|_{\boldsymbol{\nu}=\boldsymbol{\nu}_o} \tag{7.222}$$

where $\boldsymbol{\nu}_o = [u_o, 0, 0, 0, 0, 0]^\top$. Defining $\Delta\boldsymbol{\nu} := \boldsymbol{\nu} - \boldsymbol{\nu}_o$ yields

$$\dot{\boldsymbol{\eta}}_p = \Delta\boldsymbol{\nu} + \boldsymbol{\nu}_o \tag{7.223}$$

$$\boldsymbol{M}\Delta\dot{\boldsymbol{\nu}} + \boldsymbol{N}(u_o)\Delta\boldsymbol{\nu} + \boldsymbol{G}\boldsymbol{\eta}_p = \boldsymbol{\tau} + \boldsymbol{w} \tag{7.224}$$

This corresponds to a linear parameter-varying (LPV) model

$$\dot{\boldsymbol{x}} = \boldsymbol{A}(u_o)\boldsymbol{x} + \boldsymbol{B}\boldsymbol{u} + \boldsymbol{E}\boldsymbol{w} + \boldsymbol{F}\boldsymbol{\nu}_o \tag{7.225}$$

where $\boldsymbol{x} = [\boldsymbol{\eta}_p^\top, \Delta\boldsymbol{\nu}^\top]^\top$, $\boldsymbol{u} = \boldsymbol{\tau}$ and

$$\boldsymbol{A}(u_o) = \begin{bmatrix} \boldsymbol{0} & \boldsymbol{I} \\ -\boldsymbol{M}^{-1}\boldsymbol{G} & -\boldsymbol{M}^{-1}\boldsymbol{N}(u_o) \end{bmatrix}, \quad \boldsymbol{B} = \begin{bmatrix} \boldsymbol{0} \\ \boldsymbol{M}^{-1} \end{bmatrix} \tag{7.226}$$

$$\boldsymbol{E} = \begin{bmatrix} \boldsymbol{0} \\ \boldsymbol{M}^{-1} \end{bmatrix}, \quad \boldsymbol{F} = \begin{bmatrix} \boldsymbol{I} \\ \boldsymbol{0} \end{bmatrix} \tag{7.227}$$

The matrix $\boldsymbol{A}(u_o)$ depends on the forward speed u_o. This suggests that the control law for transit (maneuvering) should be gain scheduled with respect to the forward speed u_o. Notice that stationkeeping resulted in an LTI model while maneuvering implies that an LPV model must be used.

7.5.4 Transforming the Equations of Motion to a Different Point

When deriving the nonlinear equations of motion it is convenient to transform inertia, damping, gravitational and buoyancy forces between different points in $\{b\}$ to exploit structural properties of the model. For instance, the rigid-body translational and rotational parts of the system inertia matrix is decoupled if the coordinate system is located in the CG while it is common to express hydrodynamic added mass and damping in CF or a common reference point CO (see Section 2.1). This means that it is common to solve the equations of motion in three points: CG, CF and CO, all in $\{b\}$. The main tool for this is the system transformation matrix, which transforms the generalized velocities, accelerations and forces between two points in the same reference frame.

System Transformation Matrix

The system transformation matrix is derived from (3.14) for an arbitrarily point P according to

$$\begin{aligned} \boldsymbol{v}_{p/n}^b &= \boldsymbol{v}_{b/n}^b + \boldsymbol{\omega}_{b/n}^b \times \boldsymbol{r}_{p/n}^b \\ &= \boldsymbol{v}_{b/n}^b - \boldsymbol{S}\left(\boldsymbol{r}_p^b\right)\boldsymbol{\omega}_{b/n}^b \\ &= \boldsymbol{v}_{b/n}^b + \boldsymbol{S}^\top\left(\boldsymbol{r}_p^b\right)\boldsymbol{\omega}_{b/n}^b \end{aligned} \tag{7.228}$$

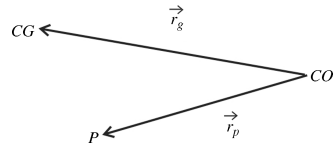

Figure 7.10 Definitions of vectors and coordinate systems.

where $\boldsymbol{r}_p^b = [x_p, y_p, z_p]^\top$ is the vector from CO to P expressed in $\{b\}$ (see Figure 7.10). For notational simplicity, we will define $\boldsymbol{r}_p^b := \boldsymbol{r}_{p/b}^b$ and $\boldsymbol{r}_g^b := \boldsymbol{r}_{cg/b}^b$.

Definition 7.3 (System Transformation Matrix)
The system transformation matrix

$$\boldsymbol{H}(\boldsymbol{r}_p^b) = \begin{bmatrix} \boldsymbol{I}_{3\times3} & \boldsymbol{S}^\top\left(\boldsymbol{r}_p^b\right) \\ \boldsymbol{0}_{3\times3} & \boldsymbol{I}_{3\times3} \end{bmatrix}, \quad \boldsymbol{H}^{-1}\left(\boldsymbol{r}_p^b\right) = \begin{bmatrix} \boldsymbol{I}_{3\times3} & \boldsymbol{S}\left(\boldsymbol{r}_p^b\right) \\ \boldsymbol{0}_{3\times3} & \boldsymbol{I}_{3\times3} \end{bmatrix} \tag{7.229}$$

transforms the linear and angular velocity vectors between the two points CO and P in the $\{b\}$ frame:

$$\begin{bmatrix} \boldsymbol{v}_{p/n}^b \\ \boldsymbol{\omega}_{b/n}^b \end{bmatrix} = \boldsymbol{H}\left(\boldsymbol{r}_p^b\right) \begin{bmatrix} \boldsymbol{v}_{b/n}^b \\ \boldsymbol{\omega}_{b/n}^b \end{bmatrix} \tag{7.230}$$

$$\Updownarrow$$

$$\boldsymbol{v}_p = \boldsymbol{H}\left(\boldsymbol{r}_p^b\right) \boldsymbol{v} \tag{7.231}$$

Similarly, the generalized force vector $\boldsymbol{\tau}$ can be transformed from CO to an arbitrary point P by

$$\begin{bmatrix} \boldsymbol{f}_b^b \\ \boldsymbol{m}_b^b \end{bmatrix} = \begin{bmatrix} \boldsymbol{f}_p^b \\ \boldsymbol{r}_p^b \times \boldsymbol{f}_p^b + \boldsymbol{m}_p^b \end{bmatrix} = \begin{bmatrix} \boldsymbol{I}_{3\times3} & \boldsymbol{0}_{3\times3} \\ \boldsymbol{S}\left(\boldsymbol{r}_p^b\right) & \boldsymbol{I}_{3\times3} \end{bmatrix} \begin{bmatrix} \boldsymbol{f}_p^b \\ \boldsymbol{m}_p^b \end{bmatrix} \tag{7.232}$$

$$\Updownarrow$$

$$\boldsymbol{\tau} = \boldsymbol{H}^\top\left(\boldsymbol{r}_p^b\right) \boldsymbol{\tau}_p \tag{7.233}$$

Matlab
The system transformation matrix is implemented in the MSS toolbox as

```
function H = Hmtrx(r)
% H = HMTRX(r) % 6x6 system transformation matrix

S = Smtrx(r);
H = [eye(3)     S'
     zeros(3,3) eye(3) ];
```

Definition 7.3 implies that the nonlinear equations of motion can be represented at an arbitrary defined point P by using the transformation matrix $\boldsymbol{H}(\boldsymbol{r}_p^b)$. Consider the nonlinear equations of motion expressed in $\{b\}$ with coordinate origin CO:

$$\boldsymbol{M}\dot{\boldsymbol{\nu}} + \boldsymbol{C}(\boldsymbol{\nu})\boldsymbol{\nu} + \boldsymbol{D}(\boldsymbol{\nu})\boldsymbol{\nu} + \boldsymbol{g}(\boldsymbol{\eta}) = \boldsymbol{\tau} \tag{7.234}$$

This expression can be transformed to a point P in $\{b\}$ by

$$\begin{aligned}\underbrace{\boldsymbol{H}^{-\top}\left(\boldsymbol{r}_p^b\right)\boldsymbol{M}\boldsymbol{H}^{-1}\left(\boldsymbol{r}_p^b\right)}_{\boldsymbol{M}_p}\dot{\boldsymbol{\nu}}_p + \underbrace{\boldsymbol{H}^{-\top}\left(\boldsymbol{r}_p^b\right)\boldsymbol{C}(\boldsymbol{\nu})\boldsymbol{H}^{-1}\left(\boldsymbol{r}_p^b\right)}_{\boldsymbol{C}_p(\boldsymbol{\nu})}\boldsymbol{\nu}_p \\ + \underbrace{\boldsymbol{H}^{-\top}\left(\boldsymbol{r}_p^b\right)\boldsymbol{D}(\boldsymbol{\nu})\boldsymbol{H}^{-1}\left(\boldsymbol{r}_p^b\right)}_{\boldsymbol{D}_p(\boldsymbol{\nu})}\boldsymbol{\nu}_p + \underbrace{\boldsymbol{H}^{-\top}\left(\boldsymbol{r}_p^b\right)\boldsymbol{g}(\boldsymbol{\eta})}_{\boldsymbol{g}_p(\boldsymbol{\eta})} = \underbrace{\boldsymbol{H}^{-\top}\left(\boldsymbol{r}_p^b\right)\boldsymbol{\tau}}_{\boldsymbol{\tau}_p}\end{aligned} \tag{7.235}$$

where

$$\boldsymbol{M}_p = \boldsymbol{H}^{-\top}\left(\boldsymbol{r}_p^b\right)\boldsymbol{M}\boldsymbol{H}^{-1}\left(\boldsymbol{r}_p^b\right) \tag{7.236}$$

$$\boldsymbol{C}_p(\boldsymbol{\nu}) = \boldsymbol{H}^{-\top}\left(\boldsymbol{r}_p^b\right)\boldsymbol{C}(\boldsymbol{\nu})\boldsymbol{H}^{-1}\left(\boldsymbol{r}_p^b\right) \tag{7.237}$$

$$\boldsymbol{D}_p(\boldsymbol{\nu}) = \boldsymbol{H}^{-\top}\left(\boldsymbol{r}_p^b\right)\boldsymbol{D}(\boldsymbol{\nu})\boldsymbol{H}^{-1}\left(\boldsymbol{r}_p^b\right) \tag{7.238}$$

$$\boldsymbol{g}_p(\boldsymbol{\eta}) = \boldsymbol{H}^{-\top}\left(\boldsymbol{r}_p^b\right)\boldsymbol{g}(\boldsymbol{\eta}) \tag{7.239}$$

From this it follows that

$$\boldsymbol{M} = \boldsymbol{H}^{\top}\left(\boldsymbol{r}_p^b\right)\boldsymbol{M}_p\boldsymbol{H}\left(\boldsymbol{r}_p^b\right) \tag{7.240}$$

$$\boldsymbol{C}(\boldsymbol{\nu}) = \boldsymbol{H}^{\top}\left(\boldsymbol{r}_p^b\right)\boldsymbol{C}_p(\boldsymbol{\nu})\boldsymbol{H}\left(\boldsymbol{r}_p^b\right) \tag{7.241}$$

$$\boldsymbol{D}(\boldsymbol{\nu}) = \boldsymbol{H}^{\top}\left(\boldsymbol{r}_p^b\right)\boldsymbol{D}_p(\boldsymbol{\nu})\boldsymbol{H}\left(\boldsymbol{r}_p^b\right) \tag{7.242}$$

$$\boldsymbol{g}(\boldsymbol{\eta}) = \boldsymbol{H}^{\top}\left(\boldsymbol{r}_p^b\right)\boldsymbol{g}_p(\boldsymbol{\eta}) \tag{7.243}$$

These expressions can be used to specify the inertia, damping and restoring forces in different reference frames in order to exploit different physical properties.

Transformation of the System Inertia Matrix

It is convenient to specify the rigid-body system inertia matrix (3.44) with respect to the CG such that

$$\boldsymbol{M}_{RB}^{cg} = \begin{bmatrix} m\boldsymbol{I}_{3\times 3} & \boldsymbol{0}_{3\times 3} \\ \boldsymbol{0}_{3\times 3} & \boldsymbol{I}_g \end{bmatrix} = \begin{bmatrix} m & 0 & 0 & 0 & 0 & 0 \\ 0 & m & 0 & 0 & 0 & 0 \\ 0 & 0 & m & 0 & 0 & 0 \\ 0 & 0 & 0 & I_x^{cg} & -I_{xy}^{cg} & -I_{zx}^{cg} \\ 0 & 0 & 0 & -I_{xy}^{cg} & I_y^{cg} & -I_{yz}^{cg} \\ 0 & 0 & 0 & -I_{zx}^{cg} & -I_{yz}^{cg} & I_z^{cg} \end{bmatrix} \tag{7.244}$$

The expression for $\boldsymbol{M}_{RB}^{cg}$ is uniquely defined by seven parameters: $\{m, I_x^{cg}, I_y^{cg}, I_z^{cg}, -I_{xy}^{cg}, -I_{zx}^{cg}, -I_{yz}^{cg}\}$. It can be transformed to the coordinate origin CO in $\{b\}$ by specifying the vector $\boldsymbol{r}_p^b = \boldsymbol{r}_g^b = [x_g, y_g, z_g]^\top$ such that the points P and CG coincide. Accordingly, (7.240) implies that

$$\boldsymbol{M}_{RB} = \boldsymbol{H}^\top\left(\boldsymbol{r}_g^b\right)\boldsymbol{M}_{RB}^{cg}\boldsymbol{H}\left(\boldsymbol{r}_g^b\right) = \begin{bmatrix} m\boldsymbol{I}_{3\times 3} & -m\boldsymbol{S}\left(\boldsymbol{r}_g^b\right) \\ m\boldsymbol{S}\left(\boldsymbol{r}_g^b\right) & \underbrace{\boldsymbol{I}_g - m\boldsymbol{S}^2\left(\boldsymbol{r}_g^b\right)}_{\boldsymbol{I}_b} \end{bmatrix}$$

$$= \begin{bmatrix} m & 0 & 0 & 0 & mz_g & -my_g \\ 0 & m & 0 & -mz_g & 0 & mx_g \\ 0 & 0 & m & my_g & -mx_g & 0 \\ 0 & -mz_g & my_g & I_x & -I_{xy} & -I_{zx} \\ mz_g & 0 & -mx_g & -I_{xy} & I_y & -I_{yz} \\ -my_g & mx_g & 0 & -I_{zx} & -I_{yz} & I_z \end{bmatrix} \tag{7.245}$$

which is recognized as (3.44).

Matlab
The 6×6 rigid-body system inertia matrix $\boldsymbol{M}_{RB}$ about an arbitrarily point o_b can be computed by using the following Matlab commands:

```
r_g = [x_g y_g z_g]'   % location of the CG w.r.t. to CO
I_g = [ Ix  -Ixy -Ixz % 3x3 inertia matrix about CG
       -Ixy  Iy  -Iyz
       -Ixz -Iyz  Iz  ]

MRB_CG = [  m*eye(3)  zeros(3,3)
          zeros(3,3)       I_g  ]

MRB = Hmtrx(r_g)'*MRB_CG*Hmtrx(r_g)
```

Transformation of the Added Mass System Inertia Matrix

Hydrodynamic seakeeping programs usually compute hydrodynamic added mass in CO or CG depending on the user specifications. Let us assume that the data have been computed in CG and that you want to

transform the result to CO, which is the point where the equations of motion are integrated numerically. The system inertia matrix $\boldsymbol{M}_A^{cg}$ is transformed to CO by choosing $\boldsymbol{r}_p^b = \boldsymbol{r}_g^b$ in (7.240). Consequently,

$$\boldsymbol{M}_A = \boldsymbol{H}^{\top}\left(\boldsymbol{r}_g^b\right)\boldsymbol{M}_A^{cg}\boldsymbol{H}\left(\boldsymbol{r}_g^b\right)$$

Next, let us assume that $\boldsymbol{M}_A$ is a diagonal matrix described by six parameters according to

$$\boldsymbol{M}_A = -\mathrm{diag}\{X_{\dot{u}}, Y_{\dot{v}}, Z_{\dot{w}}, K_{\dot{p}}, M_{\dot{q}}, N_{\dot{r}}\} \tag{7.246}$$

This is often the best estimate you have unless you are using a hydrodynamic software program that computes a full $\boldsymbol{M}_A^{cg}$ matrix (see Chapter 5). If you want to solve the equations of motion in CG instead of CO, the matrix $\boldsymbol{M}_A$ can be transformed to CG by using

$$\boldsymbol{M}_A^{cg} = \boldsymbol{H}^{-\top}\left(\boldsymbol{r}_g^b\right)\boldsymbol{M}_A\boldsymbol{H}^{-1}\left(\boldsymbol{r}_g^b\right)$$

Transformation of the Coriolis–Centrifugal Matrix

The Coriolis–centrifugal matrices are derived directly from $\boldsymbol{M}_{RB}$ and $\boldsymbol{M}_A$ by using the result in Theorem 3.2 or numerically in Matlab:

Matlab
The 6×6 Coriolis–centrifugal matrix can be computed in Matlab by using the MSS toolbox commands:

```
CA  = m2c(MA,nu)
CRB = m2c(MRB,nu)
```

Computation of the Restoring Forces and Moments

For underwater vehicles the gravitational and buoyancy forces (4.6) can be expressed in CG as

$$\boldsymbol{g}^{cg}(\boldsymbol{\eta}) = \begin{bmatrix} (W-B)\sin(\theta) \\ -(W-B)\cos(\theta)\sin(\phi) \\ -(W-B)\cos(\theta)\cos(\phi) \\ y_b B\cos(\theta)\cos(\phi) - z_b B\cos(\theta)\sin(\phi) \\ -z_b B\sin(\theta) - x_b B\cos(\theta)\cos(\phi) \\ x_b B\cos(\theta)\sin(\phi) + y_b B\sin(\theta) \end{bmatrix} \tag{7.247}$$

where x_b, y_b and z_b are the coordinates of CB with respect to CG. This expression can be transformed from CG to CO by

$$\boldsymbol{g}(\boldsymbol{\eta}) = \boldsymbol{H}^{\top}\left(\boldsymbol{r}_g^b\right)\boldsymbol{g}^{cg}(\boldsymbol{\eta}) \tag{7.248}$$

Matlab
The restoring forces and moments are generated in the MSS toolbox according to

```
g_CG = gvect(W,B,theta,phi,[0,0,0]',[xb,yb,zb]')
g    = Hmtrx(r_g)'*g_CG
```

For floating vessels the expression (4.21) can be transformed from CF to CO. In practice, it is common to assume that small angle (linear) theory holds. Hence,

$$\boldsymbol{G}^{\mathrm{cf}} = \begin{bmatrix} 0 & 0 & 0 & 0 & 0 & 0 \\ 0 & 0 & 0 & 0 & 0 & 0 \\ 0 & 0 & -Z_z & 0 & 0 & 0 \\ 0 & 0 & 0 & -K_\phi & 0 & 0 \\ 0 & 0 & 0 & 0 & -M_\theta & 0 \\ 0 & 0 & 0 & 0 & 0 & 0 \end{bmatrix} \tag{7.249}$$

Since $\boldsymbol{r}_f = [\mathrm{LCF}, 0, 0]^\top$, that is CF is located a distance LCF from CO, the restoring matrix in CO becomes

$$\begin{aligned} \boldsymbol{G} &= \boldsymbol{H}^\top \left(\boldsymbol{r}_f^b\right) \boldsymbol{G}^{cf} \boldsymbol{H} \left(\boldsymbol{r}_f^b\right) \\ &= \begin{bmatrix} 0 & 0 & 0 & 0 & 0 & 0 \\ 0 & 0 & 0 & 0 & 0 & 0 \\ 0 & 0 & -Z_z & 0 & LCF \cdot Z_z & 0 \\ 0 & 0 & 0 & -K_\phi & 0 & 0 \\ 0 & 0 & LCF \cdot Z_z & 0 & -M_\theta & 0 \\ 0 & 0 & 0 & 0 & 0 & 0 \end{bmatrix} \end{aligned} \tag{7.250}$$

Matlab

The 6×6 system spring stiffness matrix $\boldsymbol{G}$ is computed by using the MSS toolbox function Gmtrx.m:

```
A_wp = 1000          % water plane area
nabla = 10000        % displacement
GMT = 1              % transverse metacentric heights
GML = 2              % lateral metacentric heights
r_g = [1 0 10]'      % location of CG w.r.t. CO

% Spring stiffness matrix
G = Gmtrx(nabla,A_wp,GMT,GML,r_g)
```

This produces the numerical result

$$\boldsymbol{G} = \begin{bmatrix} 0 & 0 & 0 & 0 & 0 & 0 \\ 0 & 0 & 0 & 0 & 0 & 0 \\ 0 & 0 & 10055250 & 0 & -10055250 & 0 \\ 0 & 0 & 0 & 100552500 & 0 & 0 \\ 0 & 0 & -10055250 & 0 & 211160250 & 0 \\ 0 & 0 & 0 & 0 & 0 & 0 \end{bmatrix}$$

7.5.5 6 DOF Models for AUVs and ROVs

As shown in the previous sections, the 6 DOF nonlinear equations of motion can be written

$$\dot{\boldsymbol{\eta}} = \boldsymbol{J}_{\Theta}(\boldsymbol{\eta})\boldsymbol{\nu} \tag{7.251}$$

$$\boldsymbol{M}\dot{\boldsymbol{\nu}} + \boldsymbol{C}(\boldsymbol{\nu})\boldsymbol{\nu} + \boldsymbol{D}(\boldsymbol{\nu})\boldsymbol{\nu} + \boldsymbol{g}(\boldsymbol{\eta}) = \boldsymbol{\tau} \tag{7.252}$$

Note that:

$$\boldsymbol{M}_A = \boldsymbol{A}(\omega) = \text{ constant} \tag{7.253}$$

$$\boldsymbol{B}(\omega) = \boldsymbol{0} \tag{7.254}$$

for underwater vehicles operating below the wave-affected zone. The system inertia matrix $\boldsymbol{M} = \boldsymbol{M}_{RB} + \boldsymbol{M}_A$ for an underwater vehicle follows the symmetry considerations in Section 7.5.2. If we consider a starboard–port symmetrical marine craft with $y_g = I_{xy} = I_{yz} = 0$, this gives

$$\boldsymbol{M} = \begin{bmatrix} m - X_{\dot{u}} & 0 & -X_{\dot{w}} & 0 & mz_g - X_{\dot{q}} & 0 \\ 0 & m - Y_{\dot{v}} & 0 & -mz_g - Y_{\dot{p}} & 0 & mx_g - Y_{\dot{r}} \\ -X_{\dot{w}} & 0 & m - Z_{\dot{w}} & 0 & -mx_g - Z_{\dot{q}} & 0 \\ 0 & -mz_g - Y_{\dot{p}} & 0 & I_x - K_{\dot{p}} & 0 & -I_{zx} - K_{\dot{r}} \\ mz_g - X_{\dot{q}} & 0 & -mx_g - Z_{\dot{q}} & 0 & I_y - M_{\dot{q}} & 0 \\ 0 & mx_g - Y_{\dot{r}} & 0 & -I_{zx} - K_{\dot{r}} & 0 & I_z - N_{\dot{r}} \end{bmatrix}$$

Consequently, it is straightforward to compute the Coriolis and centripetal matrix $\boldsymbol{C}(\boldsymbol{\nu})$ using the results in Section 3.3 when the structure of $\boldsymbol{M}$ has been determined. In general, the damping of an underwater vehicle moving in 6 DOF at high speed will be highly nonlinear and coupled. This could be described mathematically as

$$\boldsymbol{D}_n(\boldsymbol{\nu})\boldsymbol{\nu} = \begin{bmatrix} |\boldsymbol{\nu}|^{\top}\boldsymbol{D}_{n1}\boldsymbol{\nu} \\ |\boldsymbol{\nu}|^{\top}\boldsymbol{D}_{n2}\boldsymbol{\nu} \\ |\boldsymbol{\nu}|^{\top}\boldsymbol{D}_{n3}\boldsymbol{\nu} \\ |\boldsymbol{\nu}|^{\top}\boldsymbol{D}_{n4}\boldsymbol{\nu} \\ |\boldsymbol{\nu}|^{\top}\boldsymbol{D}_{n5}\boldsymbol{\nu} \\ |\boldsymbol{\nu}|^{\top}\boldsymbol{D}_{n6}\boldsymbol{\nu} \end{bmatrix} \tag{7.255}$$

where $|\boldsymbol{\nu}| = [|u|, |v|, |w|, |p|, |q|, |r|]^{\top}$ and $\boldsymbol{D}_{ni}$ $(i = 1, \ldots, 6)$ are 6×6 matrices. Nevertheless, one rough approximation could be to use quadratic drag in surge and the cross-flow drag in sway and yaw (see Section 6.4.3). Alternatively, if the vehicle is performing a noncoupled motion, it makes sense to assume a diagonal structure of $\boldsymbol{D}(\boldsymbol{\nu})$ such that

$$\begin{aligned} \boldsymbol{D}(\boldsymbol{\nu}) = &- \text{diag}\{X_u, Y_v, Z_w, K_p, M_q, N_r\} \\ &- \text{diag}\{X_{|u|u}|u|, Y_{|vv|}|v|, Z_{|w|w}|w|, K_{|p|p}|p|, M_{|q|q}|q|, N_{|r|r}|r|\} \end{aligned} \tag{7.256}$$

Alternatively, the current coefficient representation in Section 7.3.1 can be used to model the damping. This can be done by replacing $\boldsymbol{D}_n(\boldsymbol{v})\boldsymbol{v}$ with 6 DOF current coefficients:

$$\boldsymbol{d}(V_{rc}, \gamma_{cr}) = \begin{bmatrix} -\frac{1}{2}\rho A_{F_c} C_X(\gamma_{rc}) V_{rc}^2 \\ -\frac{1}{2}\rho A_{L_c} C_Y(\gamma_{rc}) V_{rc}^2 \\ -\frac{1}{2}\rho A_{F_c} C_Z(\gamma_{rc}) V_{rc}^2 \\ -\frac{1}{2}\rho A_{L_c} H_{L_c} C_K(\gamma_{rc}) V_{rc}^2 \\ -\frac{1}{2}\rho A_{F_c} H_{F_c} C_M(\gamma_{rc}) V_{rc}^2 \\ -\frac{1}{2}\rho A_{L_c} L_{oa} C_N(\gamma_{rc}) V_{rc}^2 \end{bmatrix} \overset{\text{3DOF}}{\approx} \begin{bmatrix} -\frac{1}{2}\rho A_{F_c} C_X(\gamma_{rc}) V_{rc}^2 \\ -\frac{1}{2}\rho A_{L_c} C_Y(\gamma_{rc}) V_{rc}^2 \\ 0 \\ 0 \\ 0 \\ -\frac{1}{2}\rho A_{L_c} L_{oa} C_N(\gamma_{rc}) V_{rc}^2 \end{bmatrix} \tag{7.257}$$

where C_X, C_Y, C_Z, C_K, C_M and C_N are the current coefficients and H_{F_c} and H_{L_c} are the centroids above the water line of the frontal and lateral projected areas A_{F_c} and A_{L_c}. The 6 DOF model can also be divided into submodels, as shown in the next section.

7.5.6 Longitudinal and Lateral Models for Submarines

The 6 DOF equations of motion can in many cases be divided into two noninteracting (or lightly interacting) subsystems:

- Longitudinal subsystem: states u, w, q and θ
- Lateral subsystem: states v, p, r, ϕ and ψ

This decomposition is good for slender symmetrical bodies (large length/width ratio) or so-called "flying vehicles", as shown in Figure 7.11; typical applications are aircraft, missiles and submarines (Gertler and Hagen, 1967; Feldman, 1979; Tinker, 1982). This can also be seen from the expression of the system inertia matrix in the case of starboard–port symmetry (see Section 7.5.2):

$$\boldsymbol{M} = \begin{bmatrix} m_{11} & 0 & m_{13} & 0 & m_{15} & 0 \\ 0 & m_{22} & 0 & m_{24} & 0 & m_{26} \\ m_{31} & 0 & m_{33} & 0 & m_{35} & 0 \\ 0 & m_{42} & 0 & m_{44} & 0 & m_{46} \\ m_{51} & 0 & m_{53} & 0 & m_{55} & 0 \\ 0 & m_{62} & 0 & m_{64} & 0 & m_{66} \end{bmatrix} \tag{7.258}$$

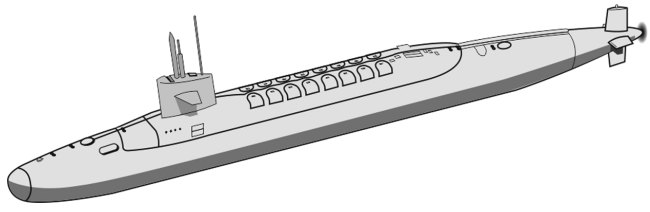

Figure 7.11 Slender body submarine (large length/width ratio).

which clearly confirms that the two subsystems

$$\boldsymbol{M}_{\text{long}} = \begin{bmatrix} m_{11} & m_{13} & m_{15} \\ m_{31} & m_{33} & m_{35} \\ m_{51} & m_{53} & m_{55} \end{bmatrix}, \quad \boldsymbol{M}_{\text{lat}} = \begin{bmatrix} m_{22} & m_{24} & m_{26} \\ m_{42} & m_{44} & m_{46} \\ m_{62} & m_{64} & m_{66} \end{bmatrix} \tag{7.259}$$

are decoupled.

Longitudinal Subsystem

Under the assumption that the lateral states v, p, r, ϕ are small, the longitudinal kinematics for surge, heave and pitch are, see (2.18) and (2.28),

$$\begin{bmatrix} \dot{D} \\ \dot{\theta} \end{bmatrix} = \begin{bmatrix} \cos(\theta) & 0 \\ 0 & 1 \end{bmatrix} \begin{bmatrix} w \\ q \end{bmatrix} + \begin{bmatrix} -\sin(\theta) \\ 0 \end{bmatrix} u \tag{7.260}$$

For simplicity, it is assumed that higher-order damping can be neglected, that is $\boldsymbol{D}_n(\boldsymbol{\nu}) = \boldsymbol{0}$. Coriolis is, however, modeled by assuming that $u \gg 0$ and that second-order terms in v, w, p, q and r are small. Hence, from (3.60) it is seen that

$$\boldsymbol{C}_{RB}(\boldsymbol{\nu})\boldsymbol{\nu} = \begin{bmatrix} m(y_g q + z_g r)p - m(x_g q - w)q - m(x_g r + v)r \\ -m(z_g p - v)p - m(z_g q + u)q + m(x_g p + y_g q)r \\ m(x_g q - w)u - m(z_g r + x_g p)v + m(z_g q + u)w \\ +(I_{yz} q + I_{xz} p - I_z r)p + (-I_{xz} r - I_{xy} q + I_x p)r \end{bmatrix}$$

such that

$$\boldsymbol{C}_{RB}(\boldsymbol{\nu})\boldsymbol{\nu} \approx \begin{bmatrix} 0 & 0 & 0 \\ 0 & 0 & -mu \\ 0 & 0 & m x_g u \end{bmatrix} \begin{bmatrix} u \\ w \\ q \end{bmatrix} \tag{7.261}$$

Notice that $\boldsymbol{C}_{RB}(\boldsymbol{\nu}) \neq -\boldsymbol{C}_{RB}^{\top}(\boldsymbol{\nu})$ for the decoupled model. Assuming a diagonal $\boldsymbol{M}_A$ as in Example 6.2, the corresponding added mass terms are

$$\boldsymbol{C}_A(\boldsymbol{\nu})\boldsymbol{\nu} = \begin{bmatrix} -Z_{\dot{w}} wq + Y_{\dot{v}} vr \\ -Y_{\dot{v}} vp + X_{\dot{u}} uq \\ (Z_{\dot{w}} - X_{\dot{u}})uw + (N_{\dot{r}} - K_{\dot{p}})pr \end{bmatrix} \approx \begin{bmatrix} 0 & 0 & 0 \\ 0 & 0 & X_{\dot{u}} u \\ 0 & (Z_{\dot{w}} - X_{\dot{u}})u & 0 \end{bmatrix} \begin{bmatrix} u \\ w \\ q \end{bmatrix} \tag{7.262}$$

According to (7.5) and (4.6) with $W = B$ and $x_g = x_b$, the dynamics becomes

$$\begin{bmatrix} m - X_{\dot{u}} & -X_{\dot{w}} & m z_g - X_{\dot{q}} \\ -X_{\dot{w}} & m - Z_{\dot{w}} & -m x_g - Z_{\dot{q}} \\ m z_g - X_{\dot{q}} & -m x_g - Z_{\dot{q}} & I_y - M_{\dot{q}} \end{bmatrix} \begin{bmatrix} \dot{u} \\ \dot{w} \\ \dot{q} \end{bmatrix} + \begin{bmatrix} -X_u & -X_w & -X_q \\ -Z_u & -Z_w & -Z_q \\ -M_u & -M_w & -M_q \end{bmatrix} \begin{bmatrix} u \\ w \\ q \end{bmatrix}$$
$$+ \begin{bmatrix} 0 & 0 & 0 \\ 0 & 0 & -(m - X_{\dot{u}})u \\ 0 & (Z_{\dot{w}} - X_{\dot{u}})u & m x_g u \end{bmatrix} \begin{bmatrix} u \\ w \\ q \end{bmatrix} + \begin{bmatrix} 0 \\ 0 \\ W\, \overline{BG}_z \sin(\theta) \end{bmatrix} = \begin{bmatrix} \tau_1 \\ \tau_3 \\ \tau_5 \end{bmatrix} \tag{7.263}$$

This model is the basis for forward speed control (state u) and depth/diving autopilot design (states w, q, θ). If the forward speed is stabilized by a forward speed controller such that

$$u = u_o = \text{constant} \tag{7.264}$$

forward speed can be eliminated from the longitudinal equations of motion such that

$$\begin{bmatrix} m - Z_{\dot{w}} & -mx_g - Z_{\dot{q}} \\ -mx_g - Z_{\dot{q}} & I_y - M_{\dot{q}} \end{bmatrix} \begin{bmatrix} \dot{w} \\ \dot{q} \end{bmatrix} + \begin{bmatrix} -Z_w & -Z_q \\ -M_w & -M_q \end{bmatrix} \begin{bmatrix} w \\ q \end{bmatrix} + \begin{bmatrix} 0 & -(m - X_{\dot{u}})u_o \\ (Z_{\dot{w}} - X_{\dot{u}})u_o & mx_g u_o \end{bmatrix} \begin{bmatrix} w \\ q \end{bmatrix} + \begin{bmatrix} 0 \\ W\,\overline{BG}_z \sin(\theta) \end{bmatrix} = \begin{bmatrix} \tau_3 \\ \tau_5 \end{bmatrix}$$

Moreover, if $\dot{w} = w = 0$ (constant depth) and θ is small such that $\sin(\theta) \approx \theta$, the linear pitch dynamics becomes

$$(I_y - M_{\dot{q}})\ddot{\theta} - M_q\dot{\theta} + W\,\overline{BG}_z\theta = \tau_5 \tag{7.265}$$

The natural frequency and period are recognized as

$$\omega_{\text{pitch}} = \sqrt{\frac{W\,\overline{BG}_z}{I_y - M_{\dot{q}}}} \tag{7.266}$$

$$T_{\text{pitch}} = \frac{2\pi}{\omega_{\text{pitch}}} \tag{7.267}$$

Lateral Subsystem

Under the assumption that the longitudinal states u, w, p, r, ϕ and θ are small, the lateral kinematics, see (7.5) and (2.28), reduce to

$$\dot{\phi} = p \tag{7.268}$$

$$\dot{\psi} = r \tag{7.269}$$

Again it is assumed that higher-order velocity terms can be neglected so that $\boldsymbol{D}_n(\boldsymbol{v}) = \boldsymbol{0}$ and that the Coriolis terms in $u = u_o$ are the most important, see (3.60),

$$\boldsymbol{C}_{RB}(\boldsymbol{v})\boldsymbol{v} = \begin{bmatrix} -m(y_g p + w)p + m(z_g r + x_g p)q - m(y_g r - u)r \\ -m(y_g q + z_g r)u + m(y_g p + w)v + m(z_g p - v)w \\ m(x_g r + v)u + m(y_g r - u)v - m(x_g p + y_g q)w \\ +(-I_{yz}q - I_{xz}p + I_z r)q + (I_{yz}r + I_{xy}p - I_y q)r \\ +(-I_{yz}r - I_{xy}p + I_y q)p + (I_{xz}r + I_{xy}q - I_x p)q \end{bmatrix}$$

Hence,

$$\boldsymbol{C}_{RB}(\boldsymbol{\nu})\boldsymbol{\nu} \approx \begin{bmatrix} 0 & 0 & mu_o \\ 0 & 0 & 0 \\ 0 & 0 & mx_g u_o \end{bmatrix} \begin{bmatrix} v \\ p \\ r \end{bmatrix} \tag{7.270}$$

Under the assumption of a diagonal $\boldsymbol{M}_A$ structure as in Example 6.2, the corresponding added mass terms are

$$\boldsymbol{C}_A(\boldsymbol{\nu})\boldsymbol{\nu} = \begin{bmatrix} Z_{\dot{w}} wp - X_{\dot{u}} ur \\ (Y_{\dot{v}} - Z_{\dot{w}})vw + (M_{\dot{q}} - N_{\dot{r}})qr \\ (X_{\dot{u}} - Y_{\dot{v}})uv + (K_{\dot{p}} - M_{\dot{q}})pq \end{bmatrix} \approx \begin{bmatrix} 0 & 0 & -X_{\dot{u}} u \\ 0 & 0 & 0 \\ (X_{\dot{u}} - Y_{\dot{v}})u & 0 & 0 \end{bmatrix} \begin{bmatrix} v \\ p \\ r \end{bmatrix} \tag{7.271}$$

Next, assume that $W = B$, $x_g = x_b$ and $y_g = y_b$. Then (7.5) and (4.6) reduce to

$$\begin{bmatrix} m - Y_{\dot{v}} & -mz_g - Y_{\dot{p}} & mx_g - Y_{\dot{r}} \\ -mz_g - Y_{\dot{p}} & I_x - K_{\dot{p}} & -I_{zx} - K_{\dot{r}} \\ mx_g - Y_{\dot{r}} & -I_{zx} - K_{\dot{r}} & I_z - N_{\dot{r}} \end{bmatrix} \begin{bmatrix} \dot{v} \\ \dot{p} \\ \dot{r} \end{bmatrix} + \begin{bmatrix} -Y_v & -Y_p & -Y_r \\ -M_v & -M_p & -M_r \\ -N_v & -N_p & -N_r \end{bmatrix} \begin{bmatrix} v \\ p \\ r \end{bmatrix}$$
$$+ \begin{bmatrix} 0 & 0 & (m - X_{\dot{u}})u \\ 0 & 0 & 0 \\ (X_{\dot{u}} - Y_{\dot{v}})u & 0 & mx_g u \end{bmatrix} \begin{bmatrix} v \\ p \\ r \end{bmatrix} + \begin{bmatrix} 0 \\ W\,\overline{BG}_z \sin(\phi) \\ 0 \end{bmatrix} = \begin{bmatrix} \tau_2 \\ \tau_4 \\ \tau_6 \end{bmatrix} \tag{7.272}$$

For vehicles where $\dot{p}$ and p are small (small roll motions) and the speed is $u = u_o$, this reduces to

$$\begin{bmatrix} m - Y_{\dot{v}} & mx_g - Y_{\dot{r}} \\ mx_g - Y_{\dot{r}} & I_z - N_{\dot{r}} \end{bmatrix} \begin{bmatrix} \dot{v} \\ \dot{r} \end{bmatrix} + \begin{bmatrix} -Y_v & -Y_r \\ -N_v & -N_r \end{bmatrix} \begin{bmatrix} v \\ r \end{bmatrix} + \begin{bmatrix} 0 & (m - X_{\dot{u}})u_o \\ (X_{\dot{u}} - Y_{\dot{v}})u_o & mx_g u_o \end{bmatrix} \begin{bmatrix} v \\ r \end{bmatrix} = \begin{bmatrix} \tau_2 \\ \tau_6 \end{bmatrix}$$

which is the sway–yaw maneuvering model (see Section 7.1.4). The decoupled linear roll equation under the assumption of a small ϕ is

$$(I_x - K_{\dot{p}})\ddot{\phi} - K_p \dot{\phi} + W\,\overline{BG}_z \phi = \tau_4 \tag{7.273}$$

From this it follows that the natural frequency and period are

$$\omega_{\text{roll}} = \sqrt{\frac{W\,\overline{BG}_z}{I_x - K_{\dot{p}}}} \tag{7.274}$$

$$T_{\text{roll}} = \frac{2\pi}{\omega_{\text{roll}}} \tag{7.275}$$